Structure of Thallium(III) Chloride, Bromide, and Cyanide Complexes in Aqueous Solution

Johan Blixt,[†] Julius Glaser,*[,†] János Mink,[†,‡] Ingmar Persson,[§] Per Persson,[∥] and Magnus Sandström*[,†]

Contribution from the Department of Chemistry, Inorganic Chemistry, The Royal Institute of Technology (KTH), S-100 44 Stockholm, Sweden, Spectroscopic Department, Institute of Isotopes of the Hungarian Academy of Sciences, P.O. Box 77, H-1525 Budapest, Hungary, Department of Chemistry, Swedish University of Agricultural Sciences, P.O. Box 7015, S-750 07 Uppsala, Sweden, and Department of Inorganic Chemistry, Umeå University, S-901 87 Umeå, Sweden

Received October 17, 1994[⊗]

Abstract: The structures of the hydrated thallium(III) halide and pseudohalide complexes, $[TlX_n(OH_2)_m]^{(3-n)+}$, X = Cl, Br, CN, in aqueous solution have been studied by a combination of X-ray absorption fine structure spectroscopy (XAFS), large-angle X-ray scattering (LAXS), and vibrational spectroscopic (Raman and IR) techniques including far-infrared studies of aqueous solutions and some solid phases with known structures. The vibrational Tl–X frequencies of all complexes are reported, force constants are calculated using normal coordinate analysis, and assignments are given. The structural results are consistent with octahedral six-coordination for the cationic complexes $Tl(OH_2)_6^{3+}$, $TlX(OH_2)_5^{2+}$, and *trans*-$TlX_2(OH_2)_4^{+}$. The coordination geometry changes to trigonal bipyramidal for the neutral $TlBr_3(OH_2)_2$ complex and possibly also for $TlCl_3(OH_2)_2$. The TlX_4^- complexes are all tetrahedral. Higher chloride complexes, $TlCl_5(OH_2)^{2-}$ and $TlCl_6^{3-}$, are formed and have again octahedral coordination geometry. For the first and second halide complexes, $TlX(OH_2)_5^{2+}$ and $TlX_2(OH_2)_4^{+}$, no lengthening was found of the Tl–X bonds, with Tl–Br distances of 2.50(2) and 2.49(2) Å, respectively, and Tl–Cl distances of 2.37(2) Å for both complexes. The mean Tl–O bond distances increase slightly, ≈0.04 Å, from that of the $Tl(OH_2)_6^{3+}$ ion, at the formation of the first thallium(III) halide complexes. A further, more pronounced lengthening of about 0.1 Å occurs when the second complex forms, and it can be related to the relatively high bond strength in the *trans*-XTlX entity, which also is manifested through the Tl–X stretching force constants. For the recently established $Tl(CN)_n^{(3-n)+}$ complexes with no previously available structural information, the Tl–C distances were determined to be 2.11(2), 2.15(2), and 2.19(2) Å for n = 2, 3, and 4, respectively. The $Tl(CN)_2^{+}$ complex has a linear structure, and the $Tl(CN)_4^-$ complex is tetrahedral with the CN^- ligands linearly coordinated. The lower complexes (n = 1–3) are hydrated, although the coordination numbers could not be unambiguously determined. A well-defined second coordination sphere corresponding to at least eight water molecules at a Tl–O[II] distance of ≈4.3 Å was found around the second complex, probably *trans*-$Tl(CN)_2(OH_2)_4^{+}$. The third cyano complex is probably pseudotetrahedral, $Tl(CN)_3(OH_2)$. The bonding in the hexahydrated Tl^{3+} and Hg^{2+} ions is discussed, and differences in the mean M–O bond lengths, determined by the LAXS and EXAFS techniques, are interpreted as being due to an occurrence of two different sets of M–O distances in the first hydration shell.

Introduction

Most chemical reactions we encounter take place in solution. Discussions of the chemical properties and reactions of the solute species, and of kinetics and mechanisms, should be based on a thorough understanding of their coordination and structure. Highly charged heavy metal ions such as thallium(III) often form very strong complexes with electron-pair donor ligands. Yet, in contrast to the detailed structures available from crystals, it is a difficult task to obtain information on the structure of such complexes in solution. Spectroscopic methods can be used for studies of symmetry and bonding properties, but diffraction techniques or EXAFS (extended X-ray absorption fine structure spectroscopy) is almost always necessary to obtain accurate interatomic metal–ligand distances.

An important but even more demanding task in this context is to determine the hydration of the species in solution. A large number of studies have been performed, and the structural properties for many hydrated metal ions are now reasonably well understood.[1] However, the situation is different concerning the coordination of water molecules to metal ions in complexes with other ligands. For this purpose we have used a combination of spectroscopic (IR/Raman and XAFS = X-ray absorption fine structure spectroscopy) and diffraction techniques (LAXS = large-angle X-ray scattering) for a systematic study of the thallium(III) chloro, bromo, and cyano complexes in aqueous solution. These complexes, which are among the strongest halide/cyanide complexes known,[2] have been extensively studied by potentiometric[2–6] and NMR spectroscopic[7,8] methods, in

[†] The Royal Institute of Technology (KTH).
[‡] Permanent address: Analytical Chemistry, University of Veszprém, P.O. Box 158, H-8201 Veszprém, Hungary.
[§] Swedish University of Agricultural Sciences.
[∥] Umeå University.
[⊗] Abstract published in *Advance ACS Abstracts,* April 1, 1995.

(1) Ohtaki, H.; Radnai, T. *Chem. Rev.* **1993**, *93*, 1157.
(2) (a) Smith, R. M.; Martell, A. F. *Critical Stability Constants*; Plenum: New York, 1977; Vol. 4. (b) Sillén, L. G.; Martell, A. E. *Stability Constants of Metal-Ion Complexes*; Special Publication Nos. 17 and 25; Chemical Society: London: 1965 and 1971. (c) Högfeldt, E. *Stability Constants of Metal-Ion Complexes*; IUPAC Chemical Data Series No. 21; Pergamon Press: Oxford, U.K., 1982; Part A, *Inorganic Ligands.*
(3) (a) Ahrland, S.; Grenthe, I.; Johansson, L.; Norén, B. *Acta Chem. Scand.* **1963**, *17*, 1567. (b) Ahrland, S.; Johansson, L. *Acta Chem. Scand.* **1964**, *18*, 2125.
(4) Woods, M. J.; Gallagher, P. K.; Hugus, Z. Z.; King, E. L. *Inorg. Chem.* **1964**, *3*, 1313.
(5) Kulba, F. Y.; Mironov, V. E.; Mavrin, I. F. *Zh. Fiz. Khim.* **1965**, *39*, 2595.

0002-7863/95/1517-5089$09.00/0

order to determine the composition and stability of the species formed. For some of the halide complexes, the structures in the solid phase as well as in solution have previously been investigated using X-ray crystallography,[9-13] LAXS on solutions,[14,15] and Raman and infrared spectroscopy.[16-18] Although these studies have revealed some general principles for the coordination chemistry of thallium(III),[9,17] it has not been possible to establish several essential structural features in the complexes $[TlX_n(OH_2)_m]^{(3-n)+}$ (X = Cl, Br, CN) formed in aqueous solution, such as the hydration numbers or the Tl−O distances of the aqua ligands.

For electrostatic reasons the interactions between the closed-shell d^{10} thallium(III) ion and the negatively charged ligands would be expected to give linear (TlX_2^+), triangular (TlX_3), tetrahedral (TlX_4^-), trigonal bipyramidal (TlX_5^{2-}), and octahedral (TlX_6^{3-}) geometries.[19] This is often consistent with the structural features found for discrete complexes in crystal structures,[20] but sometimes deviations occur due to electronic reasons. Mercury(II), an isoelectronic d^{10} ion, has a pronounced preference for two strong and short bonds in its halide and cyanide complexes,[20,21] and the Hg^{2+} ion, which is hexasolvated in many solvents including water,[22,23] generally shows an unusually large distribution of the distances to its coordinated solvent molecules in solution.[22-25] These observations have been ascribed to $5d_{z^2}$−6s mixing and second-order Jahn−Teller effects, due to near-degeneracy of the orbitals in the valence shell.[25,26] It has been suggested that similar features would occur in the coordination chemistry of the isoelectronic thallium(III) ion.[18,26]

The hydrated Tl^{3+} ion coordinates six water molecules octahedrally with a mean Tl−O bond distance of 2.17(2) Å (2.23 Å assuming a "riding" motion) in the solid compound $[Tl(OH_2)_6](ClO_4)_3$.[27] This is consistent with LAXS studies of concentrated acidic aqueous thallium(III) perchlorate solutions giving six Tl−O distances with a mean of 2.235(5) Å.[14] It has been inferred from previous NMR and LAXS studies that the hydrated TlX^{2+} and TlX_2^+ (X = Cl, Br) complexes in solution retain the octahedral geometry upon the addition of halide ligands and hence coordinate five and four water molecules, respectively.[7,14] For the $TlBr_2^+$ complex, a *trans* geometry with the Tl−Br bond distance 2.481(2) Å was established.[14] On the other hand, Spiro and Biedermann have proposed that in solution only two water molecules are coordinated to the Tl^{3+} ion, one to $TlCl^{2+}$, and none to $TlCl_2^+$.[6,18,28] Their suggestion was based on two observations: (1) the intensity of a Raman band corresponding to a proposed thallium(III)−water stretching vibration decreased linearly with added chloride and disappeared totally at a chloride/thallium ratio of 2; (2) the hydrated Tl^{3+} and $TlCl^{2+}$ species are acids whereas the higher chloride complexes are nonacidic in aqueous solution.

A LAXS study[14] on the $TlBr_3$ complex showed, in combination with crystallographic data,[9a] a planar trigonal $TlBr_3$ coordination in aqueous solution. A weak coordination of two water molecules to complete a trigonal bipyramidal structure similar to that in the solid $TlBr_3{\cdot}4H_2O$ compound was supported by the similarity of the ^{205}Tl NMR chemical shifts in solid state and in solution.[7] However, the solution structure of the $TlCl_3$ complex has been proposed to be pseudotetrahedral, $TlCl_3(OH_2)$, because of a large difference between its ^{205}Tl NMR shift in solution and an almost trigonal bipyramidal $TlCl_3(OH_2)_2$ complex in the solid state.[7,9a]

The $TlCl_4^-$ and $TlBr_4^-$ complexes are tetrahedral both in the solid state[9b,d] and in solution,[14,15] with no water molecules in the inner coordination sphere. The octahedral $TlCl_6^{3-}$ complex has been found in both the solid state[9c] and solution,[15] while the $TlCl_5(OH_2)^{2-}$, $TlBr_5(OH_2)^{2-}$, and $TlBr_6^{3-}$ species have only been ascertained in the solid state.[10,13,17]

During studies of ligand exchange and redox reactions of thallium(III) in aqueous solution,[29-31] we have encountered difficulties in proposing reaction mechanisms in cases where the structural properties of the species participating in the reactions are not known. In particular, for the ligand exchange in the Tl^{3+}−Cl^- and Tl^{3+}−Br^- systems we have proposed an unusual ligand exchange mechanism where two positively charged complex ions, for example, $Tl^{3+}(aq)$ and $TlX_2^+(aq)$, form an activated binuclear complex, $[(H_2O)_5Tl{-}X{-}Tl(OH_2)_5]^{5+}$.[29a,c] The rate-determining step for this reaction, namely, the dissociation of a water molecule from $Tl^{3+}(aq)$, allowed us to estimate the rate of water exchange for the hydrated Tl^{3+} ion. This type of reaction mechanism seems to dominate the ligand exchange in almost the entire concentration range studied.

A similar mechanism is likely also for the corresponding cyanide exchange reactions, although with a different rate-determining step.[31] No previous structural information is available for the thallium(III) cyano complexes, neither in solution nor in the solid state. Obviously, such knowledge is essential for proposing plausible reaction mechanisms and for a better understanding of the dynamics of the ligand exchange and electron-transfer reactions in solution.

The aim of the present work has been to determine the structure of the thallium(III) halide/cyanide complexes in aqueous solution and in particular the role of coordinated water molecules by using a combination of diffraction and spectro-

(6) Biedermann, G.; Spiro, T. G. *Chem. Scr.* **1971**, *1*, 155 and references therein.
(7) Glaser, J.; Henriksson, U. *J. Am. Chem. Soc.* **1981**, *103*, 6642.
(8) Blixt, J.; Györi, B.; Glaser, J. *J. Am. Chem. Soc.* **1989**, *111*, 7784.
(9) (a) Glaser, J. *Acta Chem. Scand., Ser. A* **1979**, *33*, 789; (b) **1980**, *34*, 75; (c) **1980**, *34*, 141; (d) **1980**, *34*, 157.
(10) Tuck, D. G. In *Comprehensive Coordination Chemistry*; Wilkinson, G, Gillard, R. D., McCleverty, J. A., Eds.; Pergamon: Oxford, England, 1987; Vol. 3, Chapter 25.2.8.
(11) (a) Gutierrez-Puebla, E.; Vegas, A.; Garcia-Blanco, S. *Acta Crystallogr., Sect. B* **1980**, *36*, 145. (b) Bermejo, M. R.; Castineiras, A.; Gayoso, M.; Hiller, W.; Englert, U.; Strähle, J. *Z. Naturforsch.* **1984**, *39b*, 1159.
(12) (a) Zimmermann, K.; Thiele, G. *Z. Naturforsch.* **1987**, *42b*, 818. (b) Thiele, G.; Rotter, H. W.; Faller, M. *Z. Anorg. Allg. Chem.* **1984**, *508*, 129.
(13) Glaser, J. Ph.D. Thesis, The Royal Institute of Technology (KTH), Stockholm, Sweden, 1981.
(14) Glaser, J.; Johansson, G. *Acta Chem. Scand., Ser. A* **1982**, *36*, 125.
(15) Glaser, J. *Acta Chem. Scand., Ser. A* **1982**, *36*, 451.
(16) Carr, C. Ph.D. Thesis, University of Bristol, U.K., 1984.
(17) Lee, A. G. *The Chemistry of Thallium*; Elsevier: Amsterdam, 1971 and references therein.
(18) (a) Spiro, T. G. *Inorg. Chem.* **1965**, *4*, 731; (b) **1965**, *4*, 1290; (c) **1967**, *6*, 569.
(19) (a) Deacon, C. B. *Rev. Pure Appl. Chem.* **1963**, *13*, 189. (b) Hanic, F. *K. Tek. Hoegsk. Handl.* **1972**, No. 286, 473.
(20) Wells, A. F. *Structural Inorganic Chemistry*, 5th ed.; Clarendon: Oxford, U.K., 1984; Chapters 7 and 26.
(21) Persson, I.; Sandström, M.; Goggin, P. L. *Inorg. Chim. Acta* **1987**, *129*, 183.
(22) Sandström, M.; Persson, I.; Ahrland, S. *Acta Chem. Scand., Ser. A* **1978**, *32*, 607.
(23) Åkesson, R.; Sandström, M.; Stålhandske, C.; Persson, I. *Acta Chem. Scand.* **1991**, *45*, 165.
(24) Bergström, P.-Å.; Lindgren, J.; Sandström, M.; Zhou, Y. *Inorg. Chem.* **1992**, *31*, 150.
(25) Strömberg, D.; Sandström, M.; Wahlgren, U. *Chem. Phys. Lett.* **1990**, *172*, 49.
(26) (a) Orgel, L. E. *J. Chem. Soc.* **1958**, 4186. (b) Nyholm, R. S. *J. Chem. Soc., Proc.* **1961**, 273.
(27) Glaser, J.; Johansson, G. *Acta Chem. Scand., Ser. A* **1981**, *35*, 639.
(28) Biedermann, G. *Ark. Kemi* **1953**, *5*, 441.
(29) (a) Bányai, I.; Glaser, J. *J. Am. Chem. Soc.* **1989**, *111*, 3186. (b) Henriksson, U.; Glaser, J. *Acta Chem. Scand., Ser. A*, **1985**, *39*, 355. (c) Bányai, I.; Glaser, J. *J. Am. Chem. Soc.* **1990**, *112*, 4703.
(30) (a) Blixt, J.; Dubey, R. K.; Glaser, J. *Inorg. Chem.* **1992**, *31*, 5288. (b) Blixt, J.; Glaser, J.; Solymosi, P.; Toth, I. *Inorg. Chem.* **1991**, *30*, 2824.
(31) (a) Batta, G.; Bányai, I.; Glaser, J. *J. Am. Chem. Soc.* **1994**, *116*, 3405. (b) Bányai, I.; Glaser, J. Unpublished results.

scopic techniques: LAXS, EXAFS, XANES (X-ray absorption near-edge structure), vibrational (IR and Raman), and NMR.

The LAXS method is suitable especially for determining heavy metal ion to ligand distances of complexes in concentrated solution,[32] but simultaneous determination of weakly coordinated water molecules in the inner coordination sphere can often be difficult because of overlap with other intra- and intermolecular distances in the same range, *e.g.*, O···O in the bulk water structure or in perchlorate ions. In some cases longer distances in the radial distribution functions can be easier to distinguish, *e.g.*, from a well-defined second coordination sphere of the metal ion.

In X-ray absorption fine structure spectroscopy, however, only atoms closely surrounding the absorbing element contribute significantly to the back-scattering of the ejected photoelectron. This is often advantageous, since, apart from multiple scattering, no interference occurs from distances between other atoms in the solution. Long distances, or diffuse contributions with large Debye–Waller factors, are much more rapidly damped out in the EXAFS than in the LAXS intensity functions.[33] The EXAFS technique can thus normally only be used for determinations of distinct distances within the first coordination sphere. In addition, the different shapes of the envelopes of the back-scattering amplitude for light and heavy ligand atoms can be helpful in separating their contributions to the EXAFS function.

The XANES region, which features pre-edge electronic transitions and multiple scattering resonances, is sensitive to the geometric structure of the complexes, and can provide qualitative information of value in the structural determination.[34]

Vibrational spectroscopy (infrared absorption and Raman scattering) provides information on the symmetry and bonding features of the studied complexes. The force constants obtained from normal coordinate analyses are sensitive to changes in the strength and character of the bonds and hence give the complementary information needed for a more complete structural description.[35]

NMR measurements can provide distributions and concentrations of the species present in solution, necessary for reliable interpretations of the structural data.[7,8] Also, information about the number of different ligands in a complex can often be obtained for systems in slow exchange.[8]

Experimental Section

Sample Preparation. $KTl(CN)_4$(s) was prepared from an acidic thallium(III) perchlorate stock solution (≈50 mL containing 49.03 mmol of Tl^{3+} and 173.9 mmol of H^+) kept in an ice bath, by dropwise addition with vigorous stirring of ≈35 mL of a cooled solution of potassium cyanide (205.9 mmol, ≈5% excess) and potassium hydroxide (164.1 mmol) to neutralize the acid. During the titration, a large amount of $KClO_4$ precipitated and 25 mL of water was added to facilitate stirring. After the solution was filtered, the remaining 82 mL of pale yellow-green eluate was cooled to lower the solubility of $KClO_4$. The precipitate was filtered off, and the resulting colorless solution was kept at reduced pressure over P_2O_5 until colorless crystals with the density $\varrho_{measd} = 3.07$ g cm^{-3} were obtained (see Note Added in Proof).

The thallium(III) perchlorate stock solution[13,28] and the solid compounds $[Tl(OH_2)_6](ClO_4)_3$,[27] $TlCl_3{\cdot}4H_2O$,[9a] $TlBr_3{\cdot}4H_2O$,[9a] $KTlCl_4$,[9b] $KTlBr_4{\cdot}2H_2O$,[9d] $[Co(NH_3)_6]TlCl_6$,[13] $[Co(NH_3)_6]TlBr_6$,[13] $Na_3TlCl_6{\cdot}12H_2O$,[9c] $K_3TlCl_6{\cdot}^{13}/_7H_2O$,[13] and $RbTlBr_6{\cdot}^{13}/_7H_2O$[13] were prepared as described previously. The $Tl(CN)_2^+$ solution for the LAXS measurements was prepared by adding solid KCN to the thallium(III) perchlorate stock solution and filtering off the $KClO_4$ precipitate. The $Tl(CN)_4^-$ solution for the LAXS measurements was a saturated solution of $KTl(CN)_4$. The solutions for the EXAFS and the Raman/IR measurements were prepared by adding the appropriate sodium, lithium, or potassium halide/cyanide salt to the thallium(III) perchlorate stock solution (potassium salts were used for the Raman and IR measurements in order to decrease the perchlorate concentration) or, for the $TlCl_3$ and $TlBr_3$ complexes, by dissolving the thallium(III) halide salt in water. An alternative method to prepare perchlorate-free solutions, used for the higher chloride complexes, was the addition of sodium chloride to an aqueous solution of $TlCl_3$ (obtained by oxidizing a slurry of solid TlCl with chlorine gas). To prevent reduction of thallium(III) in the bromide solutions a small amount of bromine was added. The composition of the studied solutions is given in Table 1.

Analysis. The concentration of acid in the thallium(III) solutions was determined by titration with NaOH after adding an excess of NaCl in order to prevent thallium(III) hydrolysis. The concentration of thallium(I) was determined by titration with a calibrated 0.1 M $KBrO_3$ solution using methyl orange as indicator and was found to be less than 1% of the total thallium even after 2 weeks. The total thallium content was obtained by reducing thallium(III) with SO_2, boiling off the excess SO_2, and titrating with 0.1 M $KBrO_3$.[36] In this way, the concentrations of acid, thallium(I), and thallium(III) could be determined in the same sample. The distribution of the complexes in the solutions (Table 1) was determined by ^{205}Tl NMR measurements using (a) signal integrals for slow chemical exchange on the ^{205}Tl NMR time scale and (b) the exchange-averaged chemical shifts for fast exchange on the ^{205}Tl NMR time scale (the individual chemical shifts of the $TlX_n^{(3-n)+}$ complexes were taken from previous NMR investigations[7,8]).

The crystalline $KTl(CN)_4$ salt was analyzed for potassium (by ICP) and thallium(III): found, 10.7 and 58.0%, calcd, 11.3 and 58.8%, respectively.

Large-Angle X-ray Scattering (LAXS). Measurements were carried out at ambient temperature on two concentrated solutions: one with $Tl(CN)_4^-$ and another with $Tl(CN)_2^+$ as the dominating thallium complex (*cf.* Table 1). The X-ray radiation ($\lambda_{MoK\alpha} = 0.7107$ Å) scattered from the free surface of the solutions was measured (after monochromatization in a focusing LiF crystal monochromator) as a function of the scattering angle 2θ in a $\theta-\theta$ diffractometer described previously.[32] The intensity was measured at stationary θ values with 0.1° intervals for $1° < \theta < 25°$ and 0.25° for $25° < \theta < 70°$, corresponding to the total range $0.3 < s < 16.7$ Å^{-1} of the scattering variable $s = (4\pi \sin\theta)/\lambda$. The number of counts collected twice at each point was 10^5 (corresponding to a statistical error of about 0.3%), except for $\theta < 2°$ where 4×10^4 counts were collected. The divergence of the primary X-ray beam was limited by 1°, $^1/_4$°, or $^1/_{12}$° slits for different θ regions, with overlapping data for scaling purposes. One complete set of data was collected for the $Tl(CN)_4^-$ solution, and two (which were averaged) were collected for the $Tl(CN)_2^+$ solution.

X-ray Absorption Fine Structure Spectroscopy (XAFS) Measurements. Thallium L_{III}-edge X-ray absorption data were collected in transmission mode at ambient temperature at the Stanford Synchrotron Radiation Laboratory (SSRL), Stanford University, and at the Synchrotron Radiation Source (SRS), Daresbury Laboratory, U.K., under dedicated conditions [SRS data in brackets]: 3.0 [2.0] GeV, maximum current 100 [150] mA using wiggler beamline 4-1 [wiggler station 9.2]. A Si(111) [Si(220)] double monochromator was detuned to 50% of the maximum intensity in order to reduce higher order harmonics. The solutions were kept in cells with thin glass windows (≈40 μm) and Viton spacers (1 mm). The intensity reduction by absorption in the glass windows is less than 30% at the energy range used in this study. Measurements were made on solutions with one dominating complex, typically 70% to 100% of the total thallium

(32) (a) Johansson, G. *Acta Chem. Scand.* **1966**, *20*, 553. (b) Johansson, G. *Adv. Inorg. Chem.* **1992**, *39*, 159.

(33) Persson, I.; Sandström, M.; Yokoyama, H.; Chaudhry, M. *Z. Naturforsch. A.* **1995**, *50a*, 21.

(34) (a) Bianconi, A. In *X-Ray Absorption: Principles, Applications, Techniques of EXAFS. SEXAFS and XANES*; Koningsberger, D. C., Prins, R., Eds.; Wiley-Interscience: New York, 1988; Chapter 11. (b) Sayers, D. E.; Bunker, B. A. *Ibid*; Chapter 6. (c) Fay, M. J.; Proctor, A.; Hercules, D. M. *Anal. Chem.* **1988**, *60*, 1225.

(35) Nakamoto, K. *Infrared and Raman Spectra of Inorganic and Coordination Compounds*, 4th ed.; Wiley-Interscience: New York, 1986; Chapters 2 and 3.14.

(36) Noyes, A. A.; Hoard, J. L.; Pitzer, K. S. *J. Am. Chem. Soc.* **1935**, *57*, 1231.

Table 1. Composition of the Thallium Solutions Used for Structure Determinations with Total Concentrations in mol dm^{-3} [a,b]

Solutions Used for LAXS Studies

	Tl^{3+}	CN^-	ClO_4^-	H^+	K^+	complex	% C_{Tl}
CN2a	1.43	2.82	3.95	2.48		$Tl(CN)_2^+$	97[c]
CN4a	1.50	6.01			1.51	$Tl(CN)_4^-$	>99[c]

Solutions Used for EXAFS Studies at SSRL

	Tl^{3+}	X^-	ClO_4^-	H^+	Na^+	complex	% C_{Tl}
Tl1	0.50		2.60	1.10		$Tl(OH_2)_6^{3+}$	>95[h]
Tl2	0.50		4.50	3.00		$Tl(OH_2)_6^{3+}$	>99[h]
Cl1a	0.50	0.50	3.50	2.00	0.50	$TlCl^{2+}$	80[d]
Cl2a	0.50	1.00	3.50	2.00	1.00	$TlCl_2^+$	86[d]
Cl3a	0.50	1.50	3.50	2.00	1.50	$TlCl_3$	72[d]
Cl4a	0.50	2.00	3.50	2.00	2.00	$TlCl_4^-$	97[d]
Br1a	0.50	0.50	3.50	2.00	0.50	$TlBr^{2+}$	76[d]
Br2a	0.50	1.00	3.50	2.00	1.00	$TlBr_2^+$	80[d]
Br3a	0.50	1.50	3.50	2.00	1.50	$TlBr_3$	58[d]
Br4a	0.50	2.00	2.60	1.10	2.00	$TlBr_4^-$	97[d]
CN2b	0.50	1.00	3.50	2.00	1.00	$Tl(CN)_2^+$	95[c]
CN3a	0.50	2.40	2.42	0.92	2.40	$Tl(CN)_3$	67[c]
CN4b	0.50	2.00			0.50[i]	$Tl(CN)_4^-$	>99[c]

Solutions Used for Raman and Infrared Studies[c]

	Tl^{3+}	X^-	H^+	Li^+	Na^+	complex	% C_{Tl}
Cl1b	1.35	0.70	3.00		0.70	$TlCl^{2+}$	50[f]
Cl1c	1.66	1.66	2.46			$TlCl^{2+}$	75[f]
Cl2a	0.50	1.00	2.00		1.00	$TlCl_2^+$	86[d]
Cl2b	2.14	4.27	1.59			$TlCl_2^+$	80[f]
Cl3b	3.02	9.06				$TlCl_3$	60[f]
Cl4b	3.80	15.20		3.80		$TlCl_4^-$	95[f]
Cl4c	3.02	12.10		3.04		$TlCl_4^-$	95[f]
Cl5	2.00	11.60		11.60		$TlCl_5^{2-}$	20[f,g]
Cl6	1.00	15.00		15.00		$TlCl_6^{3-}$	80[f]
Br1b	1.66	1.66	2.48			$TlBr^{2+}$	85[f]
Br2b	2.15	4.30	1.62			$TlBr_2^+$	85[f]
Br3b	3.07	9.21				$TlBr_3$	60[f]
Br4b	2.71	11.20			3.10	$TlBr_4^-$	95[f]
Br5	1.02	11.90		8.82		$TlBr_4^-$	>99[g]
CN1a	1.44	0.29	3.80		0.29	$TlCN^{2+}$	14[f]
CN1b	1.00	1.00	2.10			$TlCN^{2+}$	33[c]
CN2b	0.50	1.00	2.00		1.00	$Tl(CN)_2^+$	95[c]
CN2c	1.40	2.80	1.50			$Tl(CN)_2^+$	98[f]
CN3a	0.50	2.40	0.92		2.40	$Tl(CN)_3$	67[c]
CN3b	1.40	3.50	1.10			$Tl(CN)_3$	30[c]
CN4c	1.43	5.72			1.43[i]	$Tl(CN)_4^-$	>99[c]

[a] The thallium(I) concentration is less than 1% of the total thallium content. [b] The percentage of the complex of interest is also given. See Experimental Section. [c] Slow exchange on the ^{205}Tl NMR time scale; ^{205}Tl NMR signal integrals controlled before and after the measurements. Note that HCN is present in all H^+-containing cyanide solutions with CN/Tl ratios >2 (*cf.* Experimental Section and ref 8). [d] Fast exchange: composition estimated from the known complex distribution for 0.050 M and 1 M thallium(III) solutions (ref 7), the ^{205}Tl NMR chemical shift controlled before and after the measurements (for $TlBr_4^-$ only after the measurements) and compared to the expected shift value. [e] The concentration of ClO_4^- is omitted. [f] Estimated from complex distributions determined by NMR methods (refs 7 and 8). [g] See Results, Vibrational Spectra. [h] Estimated using the equilibrium constants from ref 28. [i] Potassium was used instead of sodium.

concentration (Table 1), and on the solid compounds $KTl(CN)_4$, $KTlCl_4$, $KTlBr_4{\cdot}2H_2O$, and $[Tl(OH_2)_6](ClO_4)_3$. The thallium concentration of the solutions, *circa* 0.5 M, was chosen to give an absorption change of about 1 logarithmic unit over the L_{III} edge for a 1 mm path. The solids were diluted with boron nitride (BN) to give a similar absorption change. Energy calibrations of the X-ray absorption spectra were performed by simultaneously recording the spectrum of a thallium foil and assigning its lowest L_{III}-edge inflection point to 12 660 eV.[37] Typically, 4–5 scans of each sample were averaged for the SSRL data, and 2–3 scans for the SRS data.

(37) *Handbook of Spectroscopy*; Robinson, J. W., Ed.; CRC Press: Boca Raton, Florida, 1991; Chapter 3.

Table 2. Large Angle X-ray Scattering: Results of Parameter Refinement From Model Fitting[a]

complex	interaction	*r*/Å	*b*/Å^2	*n*
$Tl(CN)_2^+$	Tl–C	2.11	0.002	2
	Tl–N	3.25	0.005	2
	Tl–O	2.42[b]	0.02	4
	$Tl-O^{II}$	4.3	0.09[c]	8
	Cl–O[d]	1.43	0.002[c]	4
	O···O[d]	2.335	0.008[c]	6
$Tl(CN)_4^-$	Tl–C	2.19[e]	0.0022[e]	4
	Tl–N	3.33[e]	0.0056[e]	4
	K–O	2.73	0.03	6
bulk water[c,f]	O–H	1.00	0.002	2
	O···O	2.86	0.02	1
	O···(O)···O	4.67	0.2	1

[a] *Cf.* Figure 1. *r* = interatomic distance, *b* = temperature factor coefficient ($b = 2\sigma^2$, where σ^2 is the mean square amplitude from the average distance), and *n* = number of interactions. The estimated error limits are ±0.03 Å for Tl–C, ±0.05 Å for Tl–N, and ±0.1 Å for the $Tl-O^{II}$ distances and ±0.001 Å^2 for the *b*-values of the Tl–C and Tl–N interactions. [b] From EXAFS results, Table 3. [c] Estimated values. [d] In ClO_4^-. [e] Least-squares refined values using intensity functions, *cf.* Data Treatment. [f] Used for the calculations on both $Tl(CN)_2^+$ and $Tl(CN)_4^-$.

Vibrational Spectroscopy. Raman spectra were excited using premonochromatized 514.5 nm radiation from a Coherent Radiation Laboratories Innova 90-5 argon ion laser at an effective power of approximately 500 mW at the sample. Spectra were recorded with a DILOR Z24 triple monochromator using photon counting with a spectral bandwidth of 4 cm^{-1} for the solutions and 2 cm^{-1} for the solids. Band positions are estimated to be accurate within ±1 cm^{-1}. Far-infrared spectra (range 50–500 cm^{-1}, resolution 4 cm^{-1}) were recorded with a Perkin-Elmer 1700X FTIR spectrometer as an average of 1000–10 000 scans for the aqueous solutions. Sample cells with silicon windows (Harrick) and Mylar film spacers, *circa* 17 μm were used. Concentrated (0.5–3.8 M) aqueous solutions were used, particularly for the far-infrared measurements, with compositions chosen to maximize the concentration of one complex, see Table 1. Vibrational spectra were also recorded for aqueous solutions of LiCl, $HClO_4$, and $[Tl(OH_2)_6](ClO_4)_3$ (in $HClO_4$) to be used for background subtractions. The spectra for the solid compounds $[Tl(OH_2)_6](ClO_4)_3$, $TlCl_3{\cdot}4H_2O$, $TlBr_3{\cdot}4H_2O$, $KTlCl_4$, $KTlBr_4{\cdot}2H_2O$, $KTl(CN)_4$, $[Co(NH_3)_6][TlCl_6]$, $[Co(NH_3)_6][TlBr_6]$, $Na_3TlCl_6{\cdot}12H_2O$, $K_3TlCl_6{\cdot}^{13}/_7H_2O$, and $Rb_3TlBr_6{\cdot}^{13}/_7H_2O$ were measured in a polyethene matrix, using a Nicolet 7199A FTIR system for the five latter compounds. The C–N stretching vibrations of the aqueous cyanide complexes in the mid-infrared range were covered by using solution cells with CaF_2 windows and 25 μm Teflon spacers.

NMR Measurements. ^{205}Tl NMR spectra were recorded at 230.8 MHz and at a probe temperature of 25 (±0.4) °C with a Bruker AM400 spectrometer. The NMR parameters (typically: flip angle ≈ 15°, spectral window = 125 kHz, pulse repetition time = 0.25 s, digital resolution 7.5 Hz/point) were chosen to give sufficiently quantitative (±5%) integrals and chemical shifts (±1 ppm) of the signals.

Data Treatment

Large-Angle X-ray Scattering (LAXS) Data. All calculations were carried out using the KURVLR[38] and the STEPLR[39] computer programs. The same data-reduction procedures as described previously were applied.[22,32] The structure-dependent reduced intensity function, $i(s)$, comprises contributions from all interatomic interactions in the solution. However, the oscillations originating from nonbonded intermolecular distances are rapidly damped out, and at high *s*-values only those from short, well-defined interactions remain. This allowed us to perform least-squares refinements of model parameters by fitting calculated and experimental $s{\cdot}i(s)$ curves in a suitable *s* range ($s > 5$ Å^{-1}) for the $Tl(CN)_4^-$ solution, while such refinements were not possible for the $Tl(CN)_2^+$ solution due to the high-intensity contribution from the perchlorate ion (see

(38) Johansson, G.; Sandström, M. *Chem. Scr.* **1973**, *4*, 195.
(39) Molund, M.; Persson, I. *Chem. Scr.* **1985**, *25*, 195.

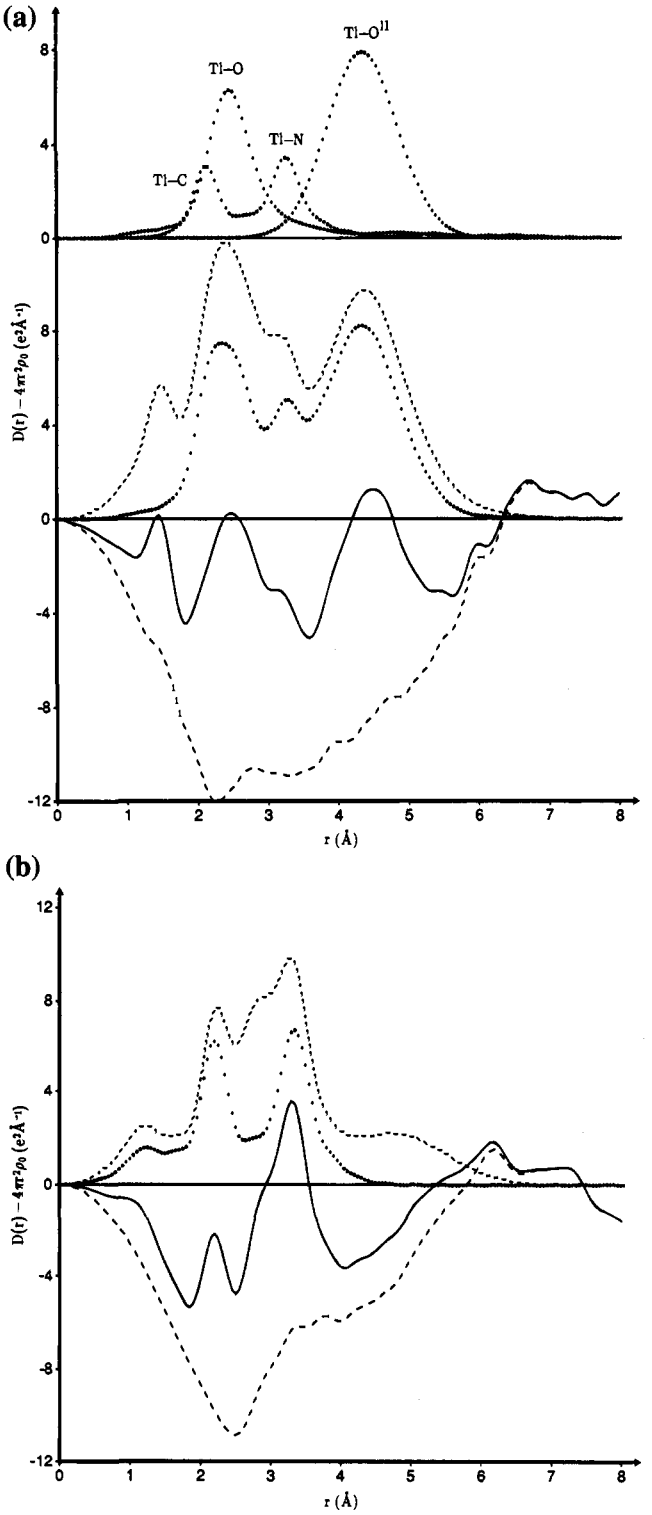

Figure 1. Large-angle X-ray scattering (LAXS) on thallium(III) cyanide solutions. Experimental reduced radial distribution functions, $D(r) - 4\pi r^2 r_0$ (—), (a) for solution CN2a and (b) for solution CN4a, together with the sum of the calculated peak shapes (- - -) and the difference between measured and calculated peak shapes (— —). The sum of all Tl–X peaks is also shown (···) and, in addition, the individual peak shapes for the Tl–X interactions (···) for the complex $Tl(CN)_2^+$.

Experimental Section). However, in the latter case Fourier transformation gives distinct peaks for the intramolecular interactions, and the model refinement for the latter solution was, instead, made on the radial distribution curve by varying the model parameters and visually comparing calculated and experimental functions until a featureless difference curve was achieved, see Figure 1a,b.

X-ray Absorption Fine Structure Spectroscopy (XAFS) Data. The EXAFS functions were extracted using standard procedures for pre-edge subtraction, spline removal, and data normalization.[34b,c] In order to obtain quantitative information, the k^3-weighted EXAFS oscillations were analyzed by a nonlinear least-squares fitting procedure of the model parameters. In the data analysis the parameters for each type of interaction (Tl–X, Tl–O) represent the mean value of all thallium complexes present in each investigated solution. The influence of the presence of minor species (*cf.* Table 1) was taken into account when estimating the error limits for the distances within the individual complexes given in Table 3.

All thallium(III) halide EXAFS data were treated using the program package EXAFSPAK,[40] where the curved-wave formalism is implemented. The k-range used in the analysis was typically 3–12 $Å^{-1}$, with the limits adjusted to the nodes of the EXAFS function. Model fitting was performed with theoretical phase and amplitude functions calculated in the single-scattering approximation with the *ab initio* code FEFF (version 5.04) of Rehr and co-workers.[41] In the theoretical calculations, the mean square deviation from the mean distance, *e.g.*, the Debye–Waller parameter σ^2, was set to 0. Therefore, the Debye–Waller parameters obtained for the complexes from the fitting procedures can be regarded as absolute values. EXAFS spectra recorded for 0.5 M solutions of the complexes $TlCl_4^-$, $TlBr_4^-$, and $Tl(OH_2)_6^{3+}$ were used to check the results obtained by using the theoretical parameters in the model refinements.

A somewhat different data analysis procedure was used for the thallium(III)–cyanide complexes due to the extensive multiple-scattering within the coordinated cyano groups.[34a,42] The phase and amplitude functions for the Tl–C and Tl–N interactions were extracted from the EXAFS data of a 0.5 M $Tl(CN)_4^-$ solution, using the distances obtained from the LAXS results. Empirical Tl–O parameters were obtained from the $Tl(OH_2)_6^{3+}$ ion in aqueous solution. All model-fitting and Fourier transform procedures were performed for k^3-weighted data, typically over the range $3.5 < k < 13.5$ $Å^{-1}$, by means of the program package XFPAKG,[43] assuming transferability of the empirical phase shift and amplitude parameters.

Vibrational Spectra. The following procedure was used to isolate the spectral features of the individual thallium(III) complexes. Spectra of water, perchloric acid (2–3 M), Tl^{3+} in acidic perchlorate solutions, and 10 M LiCl were subtracted in appropriate fractions from the spectra of the thallium solutions to eliminate medium contributions so that a relatively smooth background remained. The amounts of the different thallium complexes present in a given solution were estimated from the known complex distributions[7,8] and/or ^{205}Tl NMR spectra, and contributions from neighboring complexes were removed by spectral subtraction to isolate the features from individual complexes. All calculations and plotting were made with the program Lab Calc.[44]

NMR Spectra. The evaluation of the spectra, including integrals and chemical shifts of the signals, was performed using standard BRUKER software (DISNMR).

(40) George, G. N.; Pickering, I. J. *EXAFSPAK–A Suite of Computer Programs for Analysis of X-ray Absorption Spectra*; SSRL: Stanford, CA, 1993.

(41) (a) Rehr, J. J.; Albers, R. C.; Zabinsky, S. I. *Phys. Rev. Lett.* **1992**, *69*, 3397. (b) Rehr, J. J.; Mustre de Leon, J.; Zabinsky, S. I.; Albers, R. C. *J. Am. Chem. Soc.* **1991**, *113*, 5135. (c) Mustre de Leon, J.; Rehr, J. J.; Zabinsky, S. I.; Albers, R. C. *Phys. Rev. B* **1991**, *44*, 4146.

(42) Åkesson, R.; Persson, I.; Sandström, M.; Wahlgren, U. *Inorg. Chem.* **1994**, *33*, 3715.

(43) Scott, R. A. *Methods Enzymol.* **1985**, *117*, 414.

(44) Lab Calc; Galactic Industries Corporation, 395 Main Street, Salem, NH 03079-9891.

Table 3. Distances in $TlX_n(OH_2)_m^{(3-n)+}$ Complexes Determined by EXAFS and LAXS, Compared to the Literature Values[a]

complex	r(Tl−X)/Å	σ^2(Tl−X)/Å^2	r(Tl−O)/Å	σ^2(Tl−O)/Å^2	r(Tl−X)/Å (lit. values)	F_{fit}[b]
$Tl(OH_2)_6^{3+}$			2.21(2)	0.0064	2.235[c]	17.2
$TlCl(OH_2)_5^{2+}$	2.37	0.0037	2.24(2)	0.0095		20.4
$TlCl_2(OH_2)_4^{+}$	2.37	0.0040	2.33(4)	0.017		17.0
$TlCl_3(OH_2)_2$	2.40	0.0055	2.37(10)	0.016	2.39[d]	14.5
$TlCl_3$[e]	2.41	0.0057				17.9
$TlCl_4^-$	2.43	0.0070			2.43[f,g]	18.0
$KTlCl_4$(s)	2.42	0.0043			2.433[h]	34.5
$TlCl_5^{2-}$					2.57[i]	
$TlCl_6^{3-}$					2.59[j]	
$TlBr(OH_2)_5^{2+}$	2.50	0.0035	2.24(2)	0.0086		28.0
$TlBr_2(OH_2)_4^{+}$	2.49	0.0035	2.31(4)	0.0087	2.48[c]	27.6
$TlBr_3(OH_2)_2$	2.52	0.0039	2.34(10)	0.0220	2.51[d]	15.3
$TlBr_3$[e]	2.52	0.0039				19.4
$TlBr_4^-$	2.56[c]	0.0040			2.56[c,f]	27.5
$KTlBr_4$(s)	2.56	0.0039			2.554[k]	38.2

	r(Tl−C)/Å	$\Delta\sigma^2$(Tl−C)/Å^2	r(Tl−O)/Å	r(Tl−N)/Å
$Tl(CN)_2(OH_2)_4^{+}$	2.11	−1.6[l]	2.42(4)	3.25 (3.25[m])
$Tl(CN)_3(OH_2)$	2.15		2.42(4)	3.29
$Tl(CN)_4^-$	2.19[c]			3.33[f,m]
$KTl(CN)_4$(s)	2.19			3.33

[a] The estimated error limits in the distances determined by EXAFS are about 0.02, 0.02, and 0.03 Å for Tl−X, Tl−C, and Tl−N, respectively; for Tl−O, they are given in parentheses. For TlX_3 complexes, Tl−O interactions only marginally improve the model fit; the maximum error in the Tl−O distance is 0.1 Å. [b] Goodness of fit parameter, F_{fit}; for definition see ref 49. [c] LAXS data, ref 14. [d] Solid state $TlX_3(OH_2)_2$ species, ref 9a. [e] Calculation on unhydrated TlX_3 complex. [f] Used as model compound for the EXAFS calculations. [g] From LAXS data, ref 15. [h] $KTlCl_4$ structure, ref 9b. [i] $K_3TlCl_6 \cdot {}^{13}/_{7}H_2O$ structure, ref 13. [j] $Na_3TlCl_6 \cdot 12H_2O$ structure, ref 9c. [k] $KTlBr_4 \cdot H_2O$ structure, ref 9d. [l] Mean square amplitude relative to that of the model compound $Tl(CN)_4^-$ (in aqueous solution): $\Delta\sigma^2 = \sigma_{int}^2 - \sigma_{ref}^2$. [m] LAXS data, this work.

Results and Discussion

Large-Angle X-ray Scattering (LAXS). The Tl−C bond lengths 2.19(3) and 2.11(3) Å and the Tl−N distances 3.33(5) and 3.25(5) Å, respectively, were obtained for the $Tl(CN)_4^-$ and $Tl(CN)_2^+$ complexes, see Table 2. It was not possible to refine the parameters for coordinated water molecules in the $Tl(CN)_2^+$ complex with acceptable accuracy because of the overlapping distances from other interactions in the solution at the expected Tl−O bond distance, ≈2.4 Å. In the final model four water ligands with Tl−O distances obtained from the EXAFS results were assumed. The radial distribution functions are shown in Figure 1a,b. The final interatomic interaction parameters, used for the model calculations in Figure 1, are summarized in Table 2.

The 4.3 Å peak in the radial distribution function (Figure 1a, solid line) corresponds to at least eight water molecules in a second coordination sphere around the hydrated $Tl(CN)_2^+$ complex, but could also contain several other interactions. However, the peak is well-defined for such a long distance and corresponds to the expected metal−oxygen ($M-O^{II}$) distance for hydrogen-bonded water molecules in the second hydration sphere. Previously, $M-O^{II}$ distances of similar kind have been found at 4.0, 4.1, and 4.4 Å for the hexahydrated Rh^{3+}, Tl^{3+}, and Pb^{2+} ions (ionic radii 0.68, 0.95, and 1.27 Å), respectively.[14,45,46] In the $Tl(CN)_2(OH_2)_4^+$ complex, the Tl−OH_2 distance is 2.42 Å in the first coordination sphere (Table 3), as compared to 2.235 Å for the hydrated Tl^{3+} ion.[14] Thus, the increase in the $Tl \cdots O^{II}$ distances of about 0.2 Å from $Tl(OH_2)_6^{3+}$ to $Tl(CN)_2(OH_2)_4^+$ seems reasonable. As expected, no well-defined second coordination sphere was observed around the $Tl(CN)_4^-$ complex in solution.

The lack of structural data for the thallium(III) cyano complexes prevents comparison with the present results. The only exception is the recently published crystal structure[30b] of the compound $Na_2[Tl(edta)CN] \cdot 3H_2O$. The Tl−C bond length in this structure is 2.14(3) Å, *i.e.*, intermediate between the Tl−C distances obtained here for the $Tl(CN)_2^+$ and $Tl(CN)_4^-$ complexes, respectively. In this crystal structure the Tl−C−N coordination is almost linear (Tl−N 3.29(5) Å, Tl−C−N 171-(2)°), as also found for the solutions. However, the accuracy of the distances involving the light C and N atoms within the cyano complexes (Table 2) is not very high, especially not for the solution CN2a because of its high perchlorate concentration, *cf.* Table 1. Also the hydrogen-bonded $O \cdots O$ interactions from the bulk water structure at about 2.86 Å give a substantial background contribution for both studied solutions. The number of cyanide ligands in the complexes could not be independently determined from the X-ray data, but is known from the $^{205}Tl-{}^{13}C$ spin−spin coupling pattern in the ^{205}Tl NMR spectra of ^{13}C-enriched solutions.[8]

X-ray Absorption Near-Edge Structure (XANES). The absorption edges (XANES spectra) presented in Figure 2a−c show more or less pronounced shoulders which correspond to electronic transitions and multiple scattering resonances involving the excited 2p(Tl) electron. All the halide complexes, despite their different coordination, display two pre-edge absorption features at *circa* 12 655 and 12 668 eV. The XANES spectra of the hydrated Tl^{3+}, TlX^{2+}, and TlX_2^+ ions are qualitatively similar, with the excited states at approximately the same energies. This indicates that the octahedral coordination geometry is retained at the formation of the $TlX(OH_2)_5^{2+}$ and $TlX_2(OH_2)_4^+$ complexes. As expected for tetrahedral geometry, the pre-edge structure is very weak for the solid $KTlX_4$ compounds and for the TlX_4^- halide complexes in aqueous solution, and the spectra are almost identical (Figure 2a,b).

The complexes $Tl(CN)_n(OH_2)_m^{(3-n)+}$ ($n = 2-4$, $m = 0-4$) display two very pronounced pre-edge absorption features at *circa* 12 660 and 12 679 eV (Figure 2c). Another broad feature at about 12 696−12 708 eV increases in intensity with the number of cyanide ligands. The XANES spectra of the $Tl(CN)_4^-$ complex in the solid $KTl(CN)_4$ compound and in solution are strikingly similar.

Extended X-ray Absorption Fine Structure Spectroscopy (EXAFS). The results from the curve-fitting analysis of the

(45) Read, M. C.; Sandström, M. *Acta Chem. Scand.* **1992**, *46*, 1177.
(46) Persson, I.; Sandström, M.; Chaudhry, M. Unpublished results.

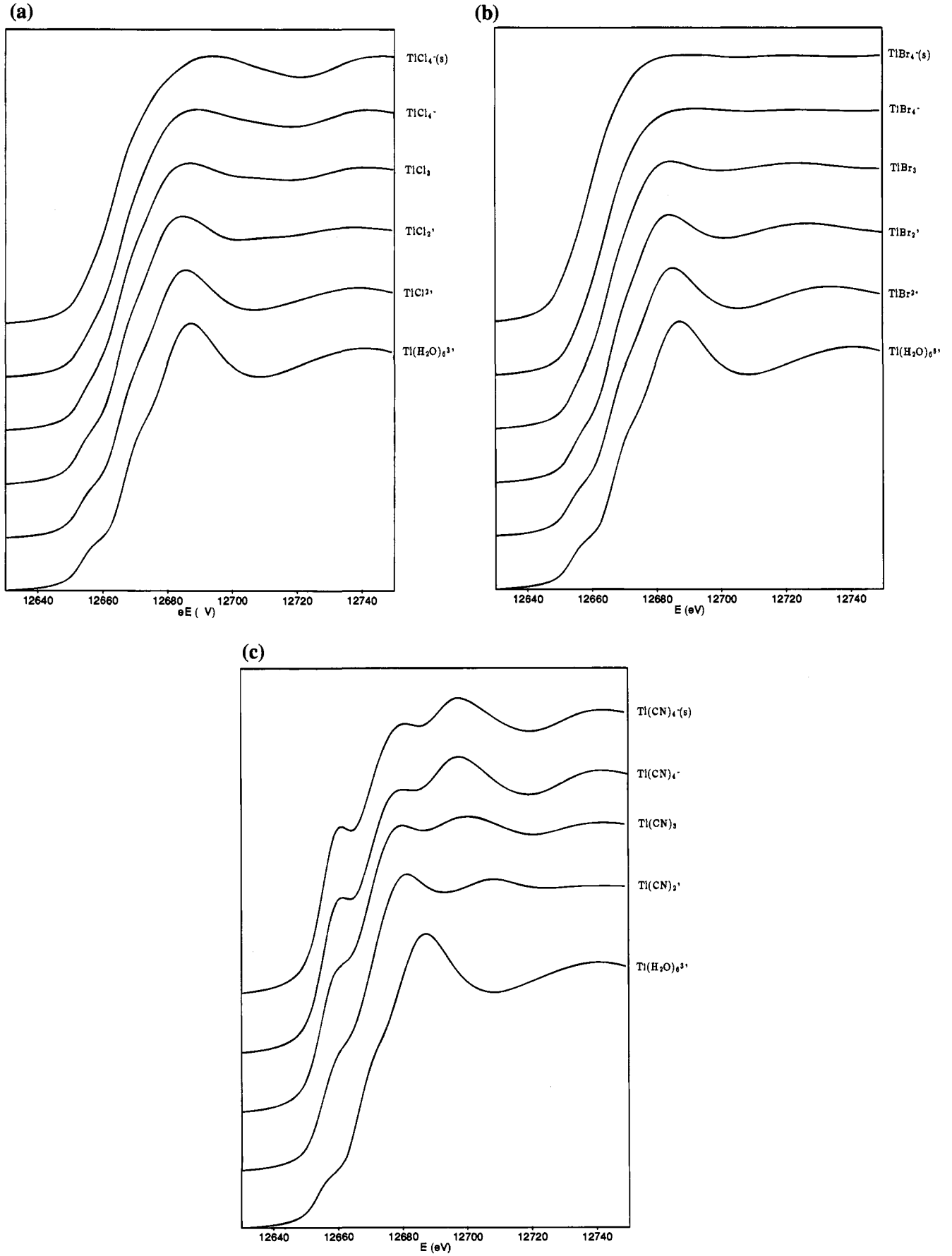

Figure 2. Absorption edges (XANES = X-ray absorption near-edge structure spectra) after calibration and normalization. Absorption edges for the $TlX_n^{(3-n)+}$ complexes in solution and for the TlX_4^- complex in the solid state: (a) X = chloride, (b) X = bromide, and (c) X = cyanide.

EXAFS data for the aqueous solutions and the solid phases are summarized in Table 3, together with results obtained from other methods for comparison. Only the SSRL results are accounted for because of problems with the beam stability during the

experiments at the SRS in Daresbury, giving less precise results in some cases. Nevertheless, no significant differences were found between the two sets of data.

As mentioned above (Data Treatment), the halide complexes were analyzed using theoretically calculated phase and amplitude data. In order to estimate the accuracy of the functions derived for the Tl−O, Tl−Cl, and Tl−Br scattering pairs and to evaluate the differences in the origin of the energy scale, ΔE_0, these functions were used to analyze the EXAFS spectra of $Tl(OH_2)_6^{3+}$(aq), $TlCl_4^-$(aq), and $TlBr_4^-$(aq). These complexes have previously been structurally characterized with the LAXS method, and both the EXAFS and the LAXS results are summarized in Table 3. As can be seen, the agreement is satisfactory.

Two acidic Tl^{3+} solutions were measured and analyzed by the EXAFS technique. Both gave a slightly shorter mean Tl−O distance (2.20−2.21 Å) than that previously obtained by the LAXS method. The shortening could not be due to partial formation of hydrolysis complexes because of the large excess of perchloric acid, particularly in the second solution (Table 1).

The least-squares refinements of the EXAFS data of the $TlX_n(OH_2)_m^{(3-n)+}$ complexes were performed by keeping the coordination numbers constant at the value of the dominating complex in each solution and varying the distances, r, and the Debye−Waller parameters, σ^2. The constant coordination numbers may introduce some additional uncertainty in the results because of the minor contributions from other complexes (see Table 1). Attempts were made to vary the coordination numbers, but because of the overlapping contributions and strong correlations the least-squares method sometimes did not result in stable parameter values. The final results are given in Table 3, and in Figure 3 the Tl−X and Tl−O contributions of the model are shown for some of the complexes. The data for the complexes $TlX(OH_2)_5^{2+}$ and $TlX_2(OH_2)_4^+$, where the Tl−O contribution is largest, are shown separately (remaining EXAFS data are given in the supplementary material). For complexes with more than one halide ligand the EXAFS pattern is dominated by the Tl−X pairs, as seen in the graphs. Consequently, the Tl−O distances obtained for the higher complexes become less well-determined, as they make only small contributions at low k-values in the TlX_3 spectra (*cf.* Figure S2 in Supplementary Material).

The reference $Tl(CN)_4^-$ solution showed two well-separated peaks 1.14 Å apart (Figure 3) in the Fourier transform of the EXAFS data, including multiple scattering, corresponding to the Tl−C and Tl−N distances which could be filtered out and back-transformed separatly (see Data Treatment). The Tl−C and Tl−N distances were evaluated from the EXAFS data on the $Tl(CN)_2^+$ and $Tl(CN)_3$ solutions and the solid $KTl(CN)_4$ compound. The distances for the $Tl(CN)_2^+$ complex were in good agreement with the LAXS results (*cf.* Tables 2 and 3).

Vibrational Spectra. Raman spectra of aqueous thallium(III) chloride and bromide solutions display a single intense polarized band in the Tl−Cl or Tl−Br stretching regions, while the Tl−O stretching bands are weak and broad features only discernible in the difference spectra. In the far-IR spectra of the aqueous solutions, after subtraction of the high background absorption from the solvent and the cell windows, relatively weak and broad Tl−X bands remain. With increasing halide/metal ratios the Raman and IR band positions move progressively toward lower wavenumbers. The spectra for each individual $TlX_n^{(3-n)+}$ complex (except the low-intensity far-IR spectra of the first TlX^{2+} complexes) obtained after spectral subtractions (see Data Treatment) are shown in Figure 4. The wavenumbers of the normal vibrations are given in Table 4, with assignments according to the proposed point group (ignoring the hydrogen atoms of the water molecules).

Six mononuclear chloro complexes are found, see Figure 4a, of which the $TlCl_5^{2-}$ complex has the degree of lowest predominance in the investigated solutions, about 20% in solution Cl5 (Table 1), as estimated from the spectral subtractions. Solution spectra of the four $TlBr_n^{(3-n)+}$ (n = 1−4) complexes are presented in Figure 4b.

For the $Tl(CN)_n^{(3-n)+}$ complexes with n = 1−4, both the Raman and the IR spectra show the CN stretching bands in the range 2200 to 2179 cm^{-1}, with decreasing frequencies for increasing coordination number (Table 4). A similar decrease is found for the metal−carbon stretching vibrations in the low-wavenumber region (Figure 4c).

Assignments of Vibrational Spectra

Halide Complexes. Results of normal-coordinate calculations have been used to support the assignments proposed in Table 4.[50a] For $TlCl^{2+}$, coinciding Raman and IR frequencies are found for the Tl−Cl and Tl−O stretching fundamentals. The weak and broad feature at about 420 cm^{-1}, Figure 4a, which probably originates from the Tl−OH_2 stretchings in the first complex, can be compared to the symmetric stretching frequency of the $Tl(OH_2)_6^{3+}$ ion, 462 cm^{-1}.[16,18] The assignment of the normal modes for the $TlX_2(OH_2)_4^+$ species (X = Cl, Br, CN) nicely follows the rule of alternative Raman or IR activity for a centrosymmetric molecule.

Normal coordinate calculations for different geometries of the TlX_3 complexes predicted an increasing separation of the symmetric and asymmetric Tl−X stretching modes when gradually transforming a pseudotetrahedral $TlX_3(OH_2)$ (C_{3v}) complex toward a trigonal bipyramidal $TlX_3(OH_2)_2$ (D_{3h}) structure.[50a] The separation increased from 3 to 15 cm^{-1} for the $TlCl_3$ unit and from 9 to 27 cm^{-1} for the $TlBr_3$ unit, as a consequence of the stronger coupling between the Tl−halide stretching modes when the three halide atoms are in the same plane. The large band separation experimentally observed in aqueous solution, 19 cm^{-1} for $TlCl_3$ and 30 cm^{-1} for $TlBr_3$, and the IR inactivity of the symmetric TlX_3 stretching mode (Table 4) suggest trigonal TlX_3 entitites for both complexes.

The interpretation of the solid state spectra is not equally straightforward. On one hand, the corresponding Tl−Br modes of the almost trigonal bipyramidal $TlBr_3(OH_2)_2$ complex in the $TlBr_3{\cdot}4H_2O$ compound at 185 (Raman) and 220 (IR) cm^{-1} (Figure 5), are close to the solution values, 190 (Raman) and 220 (IR) cm^{-1}, and thus support similar structures of the complex. On the other hand, for the isomorphous $TlCl_3{\cdot}4H_2O$ compound an unexpected closeness of the 314 cm^{-1} (Raman) and 311 cm^{-1} (IR) bands was found, which differ from the corresponding solution frequencies, 307 (Raman) and 326 (IR) cm^{-1}. In the solid compounds $TlCl_3{\cdot}4H_2O$ and $TlBr_3{\cdot}4H_2O$, asymmetric hydrogen bonds to the halide atoms are present and may shift the vibrational frequencies, particularly for the more strongly hydrogen-bonded chloride compound.[9a]

The strongly IR active frequency at 326 cm^{-1}, which should be weakly active in the Raman spectra of the $TlCl_3$ complex in solution, is consistent with a slight shoulder on the high-frequency side of the strong 307 cm^{-1} band, and is emphasized in the polarized spectrum. Likewise for $TlCl_4^-$ an asymmetry

(47) Jones, L. H. *Spectrochim. Acta*, **1963**, *19*, 1675.
(48) Jones, L. H. *Inorganic Vibrational Spectroscopy*; Marcel Dekker: New York, 1971; Chapter 4.
(49) Pickering, I. J.; George, G. N.; Damero, C. T.; Kurz, B.; Winge, D. R.; Dance, I. G. *J. Am. Chem. Soc.* **1993**, *115*, 9498.
(50) (a) Mink, J.; Mink, L.; Sandström, M. Unpublished results. (b) Carr, C.; Goggin, P. L.; Sandström, M. *J. Chem. Soc., Chem. Commun.* **1981**, 772.

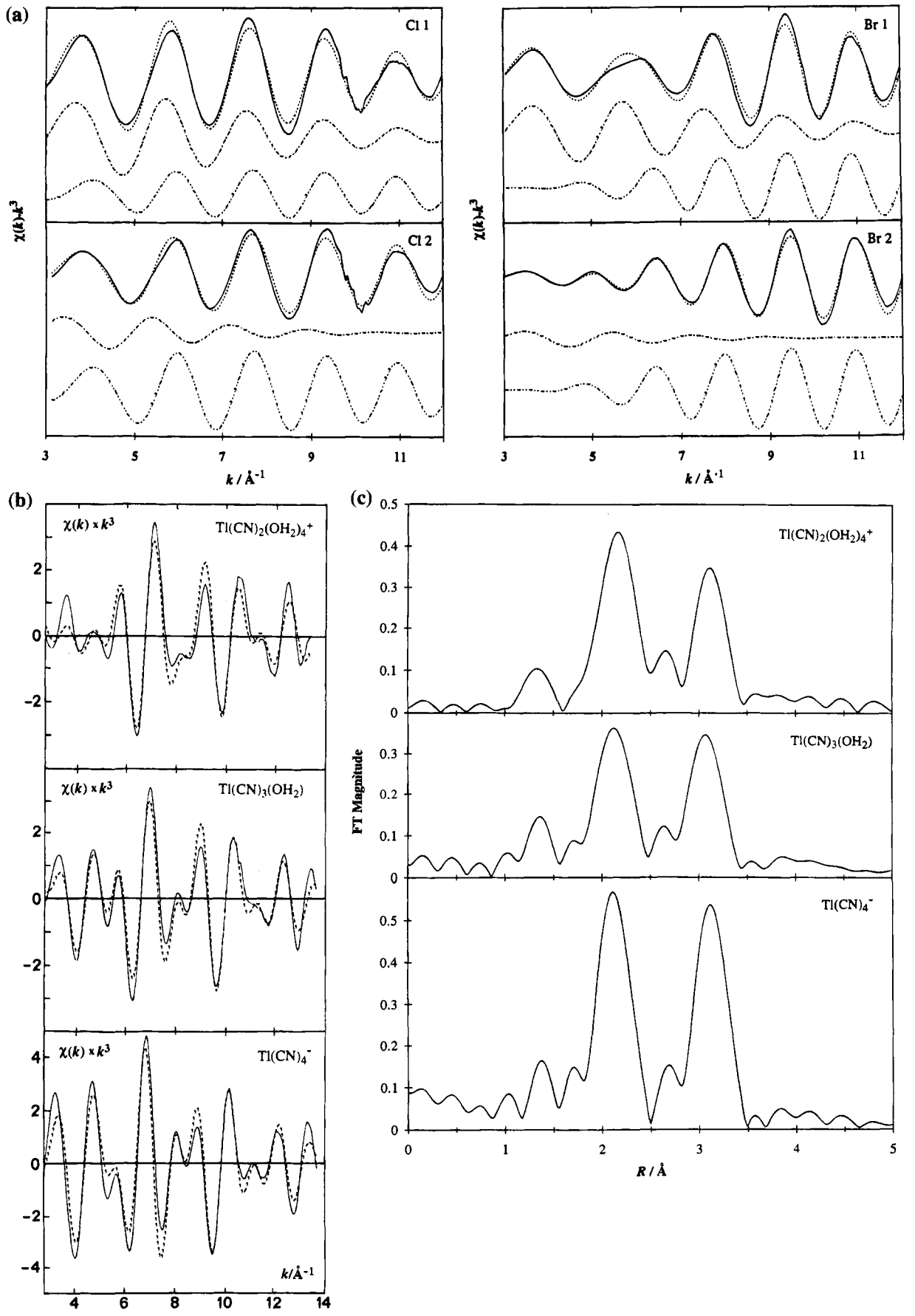

Figure 3. (a) EXAFS (extended X-ray absorption fine structure spectroscopy) model fitting of the $TlX(OH_2)_5^{2+}$ and $TlX_2(OH_2)_4^{+}$, X = Cl (solutions Cl1 and Cl2) and Br (Br1 and Br2), complexes using *ab initio* calculated parameters from FEFF.[41] The fits of the experimental $\chi(k)\cdot k^3$ function (—) and the calculated model function (- - -) using the parameters given in Table 3 are given. In addition, the individual contributions from the Tl—O (- · -) and the Tl—X (— · · —) distances are shown. (b) EXAFS model fitting of the $Tl(CN)_2(OH_2)_4^{+}$, $Tl(CN)_3(OH_2)$, and $Tl(CN)_4^{-}$ complexes using experimentally determined parameters. The fits of the experimental $\chi(k)\cdot k^3$ function (—) and the calculated function (- - -) using the parameters in Table 3 are given. (c) Fourier transform for the complexes $Tl(CN)_2(OH_2)_4^{+}$, $Tl(CN)_3(OH_2)$, and $Tl(CN)_4^{-}$ corrected for the phase shift.

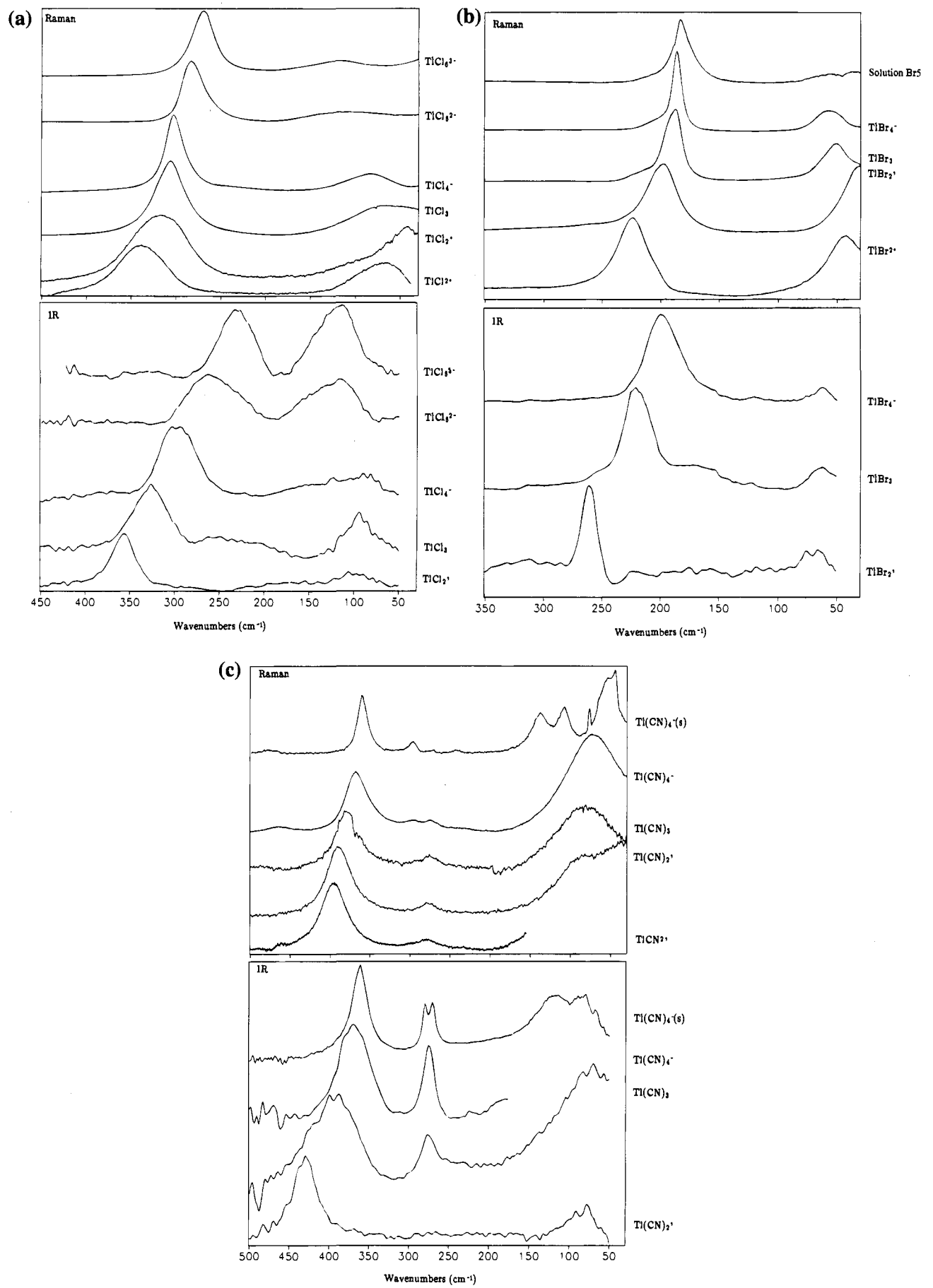

Figure 4. Raman and infrared spectra for the individual $TlX_n^{(3-n)+}$ complexes in solution for the (a) chloride, (b) bromide, and (c) cyanide complexes after spectral subtractions and background correction, see text for details. Included in panel c are also the spectra for $Tl(CN)_4^-$ in the solid compound $KTl(CN)_4$.

Table 4. Observed Vibrational Frequencies (cm^{-1}) with Proposed Assignments for Thallium(III) Complexes[a]

complex (point group)	Raman[b]	infrared[b]	assignments[a]	complex (point group)	Raman[b]	infrared[b]	assignments[a]
$TlCl(OH_2)_5^{2+}$	~420 w, sh	~420 vw, sh	E, Tl−O stretch	$TlBr_3(OH_2)_2$		~330 w	A_2'', Tl−O stretch
(C_{4v})	339 vs, pol	339 s, b	A_1, Tl−Cl stretch	(D_{3h})	~300 vw, b		A_1', Tl−O stretch
	100 sh		B_1, O−Tl−Cl deform.			257 w	
	94 m, b		E, O−Tl−Cl deform.		220 w, sh	220 vs	E', Tl−Br stretch
	69 m		E, O−Tl−O deform.		190 vs, pol		A_1', Tl−Br stretch
$TlCl_2(OH_2)_4^+$	~403 w, sh		A_{1g}, B_{1g}, Tl−O stretch			64 m, b	A_2'', O−Tl−O deform.
(D_{4h})		355 s	A_{2u}, Tl−Cl stretch		45 m		E', O−Tl−O deform.
	318 s, pol		A_{1g}, Tl−Cl stretch	$TlBr_4^-$		340 s, b	
	~110 w, sh		B_{2g}, O−Tl−O deform.	(T_d)	199 w, sh	199 s	T_2, Tl−Br stretch
		98 w, b	A_{2u}, O−Tl−Cl deform.		186 vs, pol		A_1, Tl−Br stretch
					62 sh	64 m, b	T_2, $TlBr_2$ deform.
					54 w, m		E, $TlBr_2$ deform.
$TlCl_3(OH_2)_2$	320 sh	326 s	E, Tl−Cl stretch	$Tl(CN)(OH_2)_5^{2+}$	2200 vs, pol	2199 s	A_1, C−N stretch
(D_{3h})	307 vs, pol		A_1', Tl−Cl stretch	(C_{4v})	~490 vvw		
		255 w, sh	A_2'', Tl−O stretch		450 sh		A_1, Tl−O stretch
		203 sh			400 m, s, pol		A_1, Tl−C stretch
		93 m	A_2'', O−Tl−O deform.		280 m		E, Tl−C−N bend
	67 m, b		E'', O−Tl−Cl deform.	$Tl(CN)_2(OH_2)_4^+$		2198.5	A_{2u}, C−N stretch
$TlCl_4^-$	303 vs, pol		A_1, Tl−Cl stretch	(D_{4h})	2187 vs, pol		A_{1g}, C−N stretch
(T_d)	~300 sh	296 s	T_2, Tl−Cl stretch		2149 vw		A_{1g}, ^{13}C−N stretch
	230 w, b	233 w, sh				~427 m, s	A_{2u}, Tl−O stretch
	~110 w, sh	104 m, b	T_2, $TlCl_2$ deform.		390 s, pol		A_{1g}, Tl−C stretch
	83 m, b		E, $TlCl_2$ deform.			345 s, b	A_{2u}, Tl−C stretch
$TlCl_5(OH_2)^{2-}$	~400 vvw, b		A_1, Tl−O stretch		277 w, pol		A_{1g}, Tl−O stretch
(C_{4v})	285 s, pol		A_1, $TlCl_4$ stretch			88 m, b	E_u,A_{2u}, C−Tl−O deform.
	~260 vw, sh	260 s, b	E, Tl−Cl stretch		85 m, b		E_g, C−Tl−O deform.
	135 vw, b	~135, sh	E, $TlCl_2$ deform.	$Tl(CN)_3(OH_2)$	2187 vs, pol	2188 s	A_1, E, C−N stretch
	~110, vw, b	110 s, b	E, $TlCl_2$ deform.	(C_{3v})		~425 m	A_1, Tl−O stretch
$TlCl_6^{3-}$	335 w, b					389 s	E, Tl−C stretch
(O_h)	270 s, pol		A_{1g}, Tl−Cl stretch		382 s, pol		A_1, Tl−C stretch
		230 m	T_{1u}, Tl−Cl stretch			280 w	E, Tl−C−N bend
	116 w, b		T'_{2g}, $TlCl_2$ deform.		278 m		A_1, Tl−C bend
		110 s, b	T'_{1u}, $TlCl_2$ deform.			~250 vw, b	E, Tl−C−N bend
$TlBr(OH_2)_5^{2+}$	~433 w, sh		E, Tl−O stretch			85 w, b	E, C−Tl−C deform.
(C_{4v})	350 vw, b	354 s, b	A_1,B_1, Tl−O stretch		77 w		A_1, O−Tl−C deform.
		268 vw		$Tl(CN)_4^-$	2180 vs, pol		A_1, C−N stretch
	221 s, pol	222 w	A_1, Tl−Br stretch	(T_d)	2132 vw		A_1, ^{13}C−N stretch
	190 sh					2179 s	T_2, C−N stretch
		~100 vw, b	E, O−Tl−Br deform.		472 w, b		$2\nu_9$ (T_1)
	40 m		E, O−Tl−O deform.			382 vw, sh	
$TlBr_2(OH_2)_4^+$		~336 w, b	E_u, Tl−O stretch		368 s, pol		A_1, Tl−C stretch
(D_{4h})	~320 vw, b		A_{1g}, Tl−O stretch			368 m	T_2, Tl−C stretch
		261 vs	A_{2u}, Tl−Br stretch				
	198 vs, pol		A_{1g}, Tl−Br stretch		345 vw, sh		A_1, Tl−^{13}C stretch
		65 s, b	A_{2u}, O−Tl−Br deform.		297 w		E, Tl−C−N bend
	30 m		E_g, O−Tl−Br deform.		275 w	275 m	T_2, Tl−C−N bend
					232 vw		T_1, Tl−C−N bend
						~130 w, b	$2\nu_8$ (T_2)
					70 s, b		E, C−Tl−C deform.

[a] Symmetry species are given in the point group obtained by ignoring the hydrogen atoms. [b] Abbreviations: b = broad, m = medium, p = polarized, s = strong, sh = shoulder, v = very, w = weak.

on the low-frequency side of the strong $\nu_1(A_1)$ Raman band at 303 cm^{-1} corresponds to the strongly IR active ν_3 band at 296 cm^{-1}. The Raman spectrum of the tetrahedral $TlCl_4^-$ ions in the solid $KTlCl_4$ is shown in Figure 5 and has a similar appearance with a shoulder at 293 cm^{-1} on the main 299 cm^{-1} band.

The shoulder on the low-frequency side of the strong Raman band at 285 cm^{-1} for the $TlCl_5(OH_2)^{2-}$ complex corresponds to the IR active band at 260 cm^{-1}. An IR absorption band at 262 cm^{-1} was reported previously for the $TlCl_5^{2-}$ complex in aqueous solution, but no conclusion could then be drawn about its structure.[50b] The Raman spectra of the solid compounds $Rb_2TlCl_5(OH_2)$ and $(NH_4)_2TlCl_5{\cdot}H_2O$, which have been reported to contain $TlCl_5(OH_2)^{2-}$ complexes,[18b] give strong Raman bands at 294 and 286 cm^{-1}. In the solid compound $K_3TlCl_6{\cdot}^{13}/_7H_2O$, which contains one $TlCl_5(OH_2)^{2-}$ and two $TlCl_6^{3-}$ species,[13] the Raman bands occurring at 280 and 262 cm^{-1} probably originate from the two different types of complexes, respectively. The solid $[Co(NH_3)_6][TlCl_6]$ compound displays a strong Raman band at 264 cm^{-1} which corresponds to the $A_{1a}(O_h)$ frequency of $TlCl_6^{3-}$ and an IR active $T_{1u}(O_h)$ band at ≈207 cm^{-1}. The $TlCl_6^{3-}$ complex in the $Na_3TlCl_6{\cdot}12H_2O$ structure with all six Tl−Cl distances equal, 2.593(3) Å, is extensively hydrogen bonded to the water molecules[9c] and has a symmetric Raman stretching frequency at 276 cm^{-1}. In solution, the corresponding Raman band occurs at 270 cm^{-1} and the IR band at 230 cm^{-1}. Evidently, the environment and the hydrogen bonding in the solid can cause considerable shifts in the vibration frequencies of the chloride complexes.

The stretching force constants K(Tl−X) have been evaluated for the first four complexes (Table 5),[50a] and are clearly correlated with the Tl−X bond lengths (Figure 6a). The high bond strength for the *trans*-TlX_2^+ entity compared to TlX^{2+} is obvious, particularly for the $TlBr_2^+$ species where the bond strength is even higher than in $TlBr^{2+}$. This supports the trends in the Tl−X distance variations obtained from the EXAFS results (Table 3).

A search was made for bromide complexes higher than $TlBr_4^-$ in solution. Subtraction of the Raman spectrum of the $TlBr_4^-$

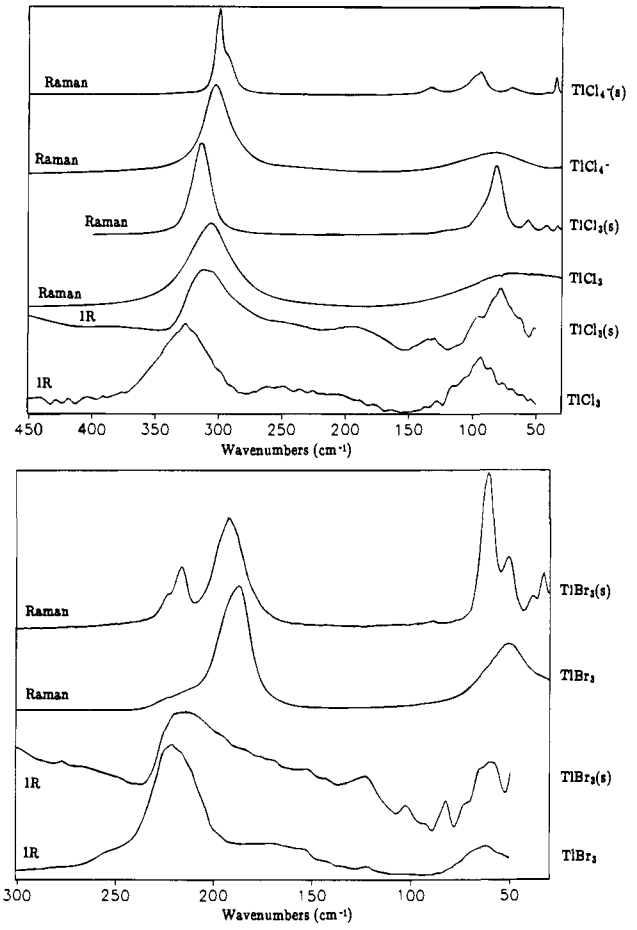

Figure 5. Raman and infrared spectra for the individual complexes $TlBr_3$, $TlCl_3$, and $TlCl_4^-$ in solution and in the solid compounds $TlBr_3{\cdot}4H_2O$, $TlCl_3{\cdot}4H_2O$, and $KTlCl_4$. For $TlBr_3{\cdot}4H_2O$, only a few IR scans could be recorded before decomposition occured.

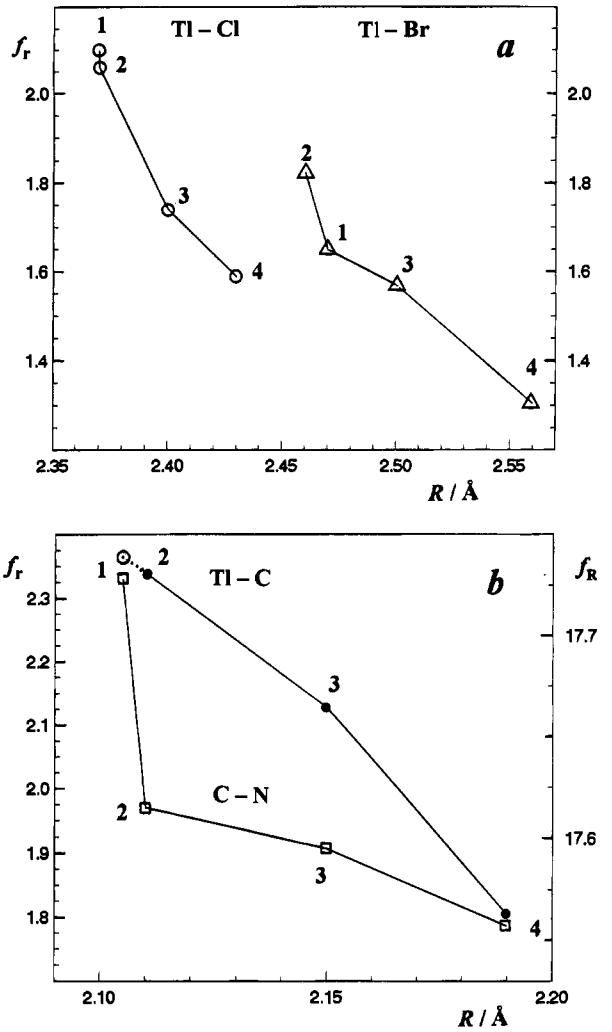

Figure 6. Correlations between bond distances (Å) and stretching force constants f (N cm^{-1}), see Table 5, for (a) thallium(III) halide $TlX_n^{(3-n)+}$ (n = 1–4 and X = Cl (○), Br (△)) and (b) thallium(III) cyanide complexes $Tl(CN)_n^{(3-n)+}$ (n = 1–4), with the Tl–C bond length versus force constant f_r (●, left-side scale) extrapolated for the first complex (○) and the C–N bond versus force constant f_R (□, right-side scale).

complex from a spectrum of a thallium(III) solution with a free bromide concentration of ≈7.8 M gave a remaining low-intensity band at 183 cm^{-1} (Figure 4b). The Raman and IR spectra of the hydrated salt $Rb_3TlBr_6{\cdot}^{13}/_7H_2O$, which contains both $TlBr_5(OH_2)^{2-}$ and $TlBr_6^{3-}$ complexes,[13] gave the following Tl–Br stretching frequencies: Raman 174 (s), 164 (vs), 156 (vs) cm^{-1}; IR 190 (m), 158 (s), 139 (s) cm^{-1}. The compound $[Co(NH_3)_6][TlBr_6]$ has a strong Raman band at 159 cm^{-1} and IR bands at 204 (weak) and at 145 (strong) cm^{-1}.[18] Therefore, we assign the 174 cm^{-1} band for $Rb_3TlBr_6{\cdot}^{13}/_7H_2O$ to the $TlBr_5(OH_2)^{2-}$ complex. The observed shift in solution of only 3 cm^{-1} for the residual minor 183 cm^{-1} band from the major 186 cm^{-1} band of the tetrahedral $TlBr_4^-$ complex is thus too small to correspond to a $TlBr_5(OH_2)^{2-}$ complex in solution, particularly as the shift between the $TlCl_4^-$ and $TlCl_5(OH_2)^{2-}$ complexes is 18 cm^{-1} (Table 4), and a ratio of about ν(M–Br)/ν(M–Cl) = 0.6 would be expected for the stretching vibrations.[35] We propose that the weak 183 cm^{-1} band originates from a partial ion-pair formation between the $TlBr_4^-$ complex and Li^+ ions in this concentrated solution saturated with LiBr. This could also explain the slight increase in the

Table 5. Correlation Between the Symmetric Stretching Force Constants, K/(N cm^{-1}), and the Metal–Ligand Bond Distances, r/Å, for Thallium(III) and Mercury(II) Complexes in Aqueous Solution

complex	K(M–X)	K(C≡N)	r	complex	K(M–X)	K(C≡N)	r
$TlCl^{2+}$	2.099		2.37				
$TlCl_2^+$	2.061		2.37	$HgCl_2$	2.530		2.29[a]
$TlCl_3$	1.741		2.40	$HgCl_3^-$			2.45[b]
$TlCl_4^-$	1.588		2.43	$HgCl_4^{2-}$			2.47[b]
$TlBr^{2+}$	1.649		2.50				
$TlBr_2^+$	1.823		2.49	$HgBr_2$	2.246		2.42[a]
$TlBr_3$	1.570		2.52	$HgBr_3^-$			2.58[c]
$TlBr_4^-$	1.305		2.56	$HgBr_4^{2-}$			2.61[c]
$Tl(CN)^{2+}$	2.364	17.73	~2.10[d]				
$Tl(CN)_2^+$	2.339	17.62	2.11	$Hg(CN)_2$	2.519	18.20	2.04[a]
$Tl(CN)_3$	2.127	17.60	2.15	$Hg(CN)_3^-$			2.14[e]
$Tl(CN)_4^-$	1.804	17.56	2.19	$Hg(CN)_4^{2-}$	1.53[f]	17.08[f]	2.20[g]

[a] Reference 42. [b] Reference 55b. [c] Reference 51. [d] Predicted from force constant values, see Figure 6. [e] Reference 57. [f] References 47 and 48. [g] Reference 54.

Tl−Br distance (≈0.02 Å) which previously has been found by the LAXS method when adding a large excess of Li^+ to a $TlBr_4^-$ solution.[14]

Cyanide Complexes. The assignments given for the thallium(III) cyanide complexes are based on comparisons with the analogous complexes of the isoelectronic mercury(II) ion,[47,48] and on results of normal coordinate calculations.[50a] For the $Tl(CN)_3$ and $Tl(CN)_4^-$ complexes some discussion is needed. We have calculated the fundamental frequencies of a $Tl(CN)_3(OH_2)$ complex for pseudotetrahedral (C_{3v}) and square-planar (C_{2v}) symmetries and for $Tl(CN)_3(OH_2)_2$ in trigonal-bipyramidal (D_{3h}) symmetry. As for the halide complexes the splitting of the Tl−C frequencies was strongly geometry dependent. The calculated separation between the Tl−C asymmetric and symmetric stretching bands was found to be 15, 39, and 40 cm^{-1} for the assumed C_{3v}, C_{2v}, and D_{3h} symmetries, respectively. The experimentally observed separation is only 7 cm^{-1}, which is closest to the pseudotetrahedral model.

Generally, square-planar tetracyano metal complexes show higher metal−carbon stretching wavenumbers and stronger bonds than tetrahedral complexes.[47,48] For example, the Au−C stretching force constant of the $Au(CN)_4^-$ complex is 2.78 N cm^{-1}, which is considerably higher than the corresponding value for the $Tl(CN)_4^-$ complex (Table 5). Also, for the $Tl(CN)_4^-$ complex the near coincidence of the Raman and IR stretching frequencies indicates little interaction between the cyano ligands, as expected for a tetrahedral arrangement, in contrast to the splitting of 18 cm^{-1} for $Au(CN)_4^-$.[42,47,48]

The Tl−C stretching frequency decreases with an increasing number of cyano ligands (Table 4), although particularly the stretching force constants reveal a relatively high Tl−C bond strength in the $Tl(CN)_2^+$ complex. The correlation between the Tl−C bond distances and stretching force constants is shown in Figure 6b and allows an estimation of a Tl−C bond length of about 2.10 Å for the $Tl(CN)(OH_2)_5^{2+}$ complex (Table 5).

Also the C−N stretching force constant decreases with an increasing number of cyano ligands (Table 5), indicating a weakened C−N bond. The effect has been explained in similar complexes as being due to a less symmetrical and, thus, weaker bond in the CN ligand when the metal−carbon bond strength decreases and reduces the polarization of the C−N bond toward the carbon atom. However, more covalent M−C bonding with an increasing charge-transfer leads to a higher amount of π-back-bonding and also weakens the CN bonds, since the back-bonding electrons enter into an antibonding π^* orbital.[47,48]

For the linear $Tl(CN)_2^+$ complex the weakening indicated in the C−N bonds is more pronounced than expected when the Tl−C and the C−N correlations (Figure 6b) were compared. This suggests a higher degree of back-bonding from the thallium atom than in the other thallium complexes. The $Tl(CN)_4^-$ complex has higher M−C and C−N stretching force constants than $Hg(CN)_4^{2-}$ (Table 5), as expected from the higher oxidation state of the thallium(III) atom. However, for the $Tl(CN)_2^+$ complex both these force constants have *lower* values than for $Hg(CN)_2$, which is consistent with the higher degree of covalency in the Hg−C bonds and the stronger back-bonding (*cf.* discussion in ref 42). The relatively high charge retained at the thallium atom corresponds to its fairly strong hydration, while the anomalously strong Hg−C σ-bonding in the $Hg(CN)_2$ complex gives a lower charge and a much weaker hydration.[42] Further investigations of the bonding in these systems are in progress.

Structures of the Hydrated $TlX_n^{(3-n)+}$ Complexes

Summarizing all available information on the halo and cyano complexes of thallium(III), the following structures can be proposed in aqueous solution (Figure 7).

$Tl(OH_2)_6^{3+}$. Both the previous LAXS study and the present EXAFS results showed that the Tl^{3+} ion is surrounded by six water molecules. However, as discussed below (Acidity and Water Coordination), there is a slight difference in the Tl−O distances obtained with the two techniques, which indicates some distortion of the octahedral coordination geometry.

TlX^{2+}. When the first halide ligand is coordinated, five water molecules remain bonded to the thallium atom. The average Tl−O distance increases slightly, *circa* 0.04 Å, as compared to that of $Tl(OH_2)_6^{3+}$, and the Tl−O stretching vibration decreases by 30−40 cm^{-1} (Table 4). Even though only a single Tl−O distance can be distinguished, it is possible that the water molecule *trans* to the halide ligand is somewhat more strongly bonded to the thallium atom (the present EXAFS data do not allow better resolution than 0.1 Å).

TlX_2^+. The vibrational spectra (see above) show that the XTIX unit has *trans* geometry. For the $TlBr_2^+$ complex, this is confirmed by the Br−Br distance determined from LAXS data.[14] Four water molecules at a Tl−O bond length of ≈2.3 Å presumably complete an octahedral coordination (*cf.* Table 3). The Tl−X bond distance remains almost unchanged upon the formation of the TlX_2^+ complex from the TlX^{2+} (X = Cl, Br) species, and the Tl−OH_2 bond length increases considerably, ≈0.1 Å. This is probably due to a strong decrease of the positive charge of the metal ion at the coordination of the second X ligand, consistent with the increasing Tl−O bond distance in the order Cl < Br < CN (thus an increase with increasing softness/polarizability of the ligand X). The pronounced weakening of the Tl−O bond strength is reflected in the very weak and broad IR/Raman bands (*cf.* Table 4). The variation of the Tl−X bond strength at the stepwise complex formation is shown in a more sensitive way by the stretching force constants than by the changes of the distances (Table 5 and Figure 6).

The linearity of the second cyano complex, $Tl(CN)_2^+$, is expected since other d^{10} metal ions, *e.g.*, copper(I), silver(I), gold(I), and mercury(II), also form linear dicyano complexes.[20,47,48] As mentioned above (Results and Discussion, LAXS), there is strong evidence for a second coordination sphere comprising approximately eight water molecules at a Tl−O^{II} distance of 4.3 Å. This can be rationalized by assuming two H_2O^{II} molecules hydrogen bonded to each of the water molecules of the first hydration sphere of an assumed $Tl(CN)_2(OH_2)_4^+$ complex.

TlX_3. In the case of the bromo complex there is direct evidence of an approximately trigonal-planar $TlBr_3$ unit in solution, namely, the ratio of the distances $r_{Br-Br}/r_{Tl-Br} = 1.74$ (±0.02) (expected $\sqrt{3}$) obtained from LAXS data.[14] Moreover, the IR/Raman spectra are compatible with D_{3h} symmetry for both the $TlBr_3(OH_2)_2$ and $TlCl_3(OH_2)_2$ species in solution. However, the Tl−O distances determined in this work are somewhat uncertain because of their small contribution to the EXAFS spectra. For the tricyano complex, a pseudotetrahedral C_{3v} symmetry for a species $Tl(CN)_3(OH_2)$ seems likely (see Assignments of Vibrational Spectra). Although the model fitting for the EXAFS spectra could not distinguish between one or two water ligands, a distinct Tl−O bond length (2.42 Å, Table 3) was obtained. In the solid state, somewhat distorted trigonal-bipyramidal TlX_3O_2 units with long (2.4−2.6 Å) Tl−O distances and the thallium atoms slightly above the X_3 plane exist in the compounds $TlCl_3{\cdot}4H_2O$,[9a] $TlBr_3{\cdot}4H_2O$,[9a] $TlCl_3(3\text{-}CN_3C_5H_4NO)_2$,[11a] and $TlI_3(3\text{-}CH_3C_5H_4NO)_2$.[11b]

However, a comparison between the ^{205}Tl NMR shifts for the solid compounds $TlX_3{\cdot}4H_2O$, 2051 ppm for X = Cl and 1098 ppm for X = Br, and the individual chemical shifts of the TlX_3 complexes in solution, 2412 ppm for X = Cl and 1184

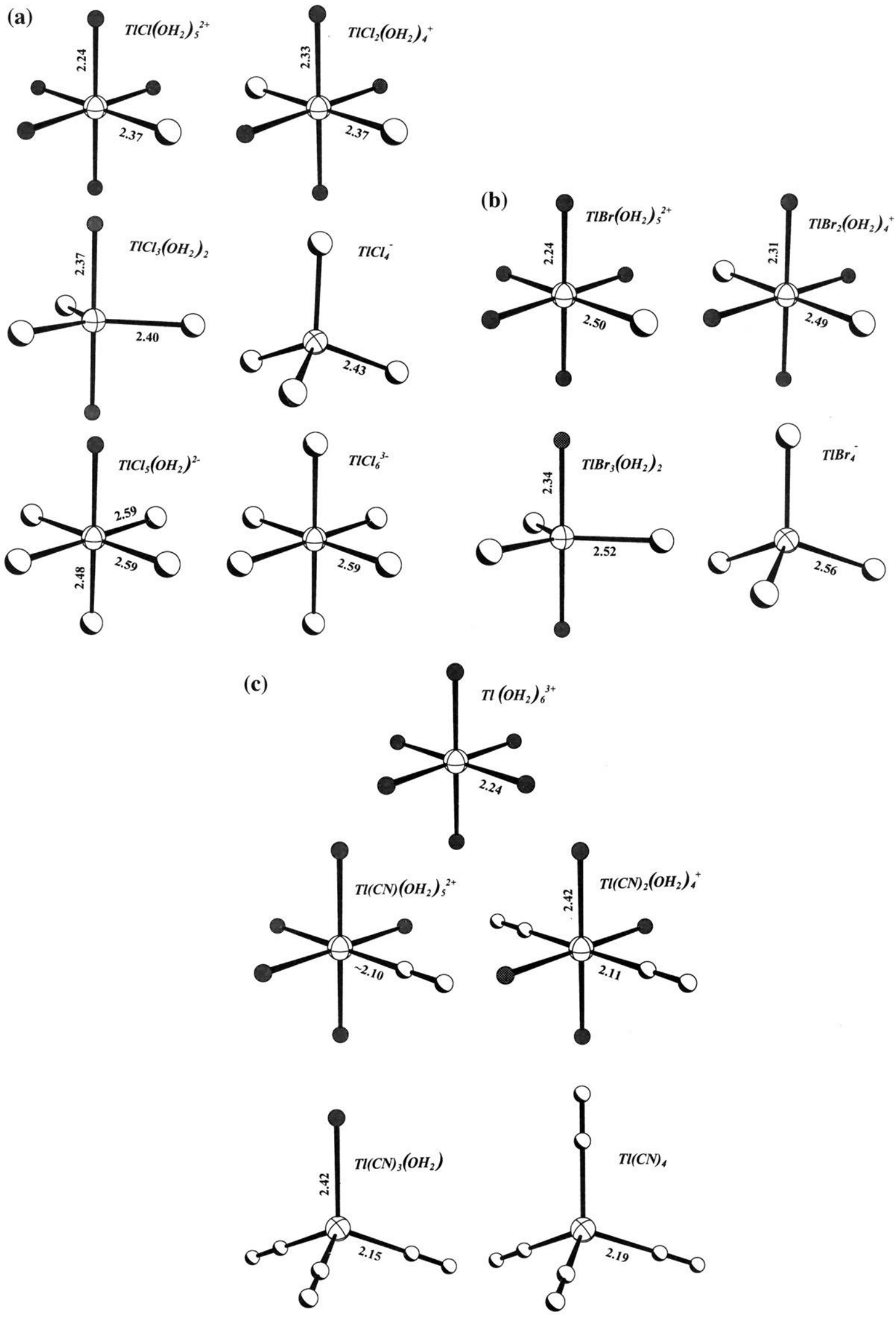

Figure 7. Proposed structures and the determined interatomic distances, in Å, for the (a) thallium(III) chloro, (b) bromo, and (c) cyano complexes in aqueous solution; for details see text and Table 3. The water oxygen atoms are dark, whereas the Br, Cl, C, and N atoms are shaded.

ppm for X = Br,[7] indicates a larger change in the chemical surrounding of the thallium atom in the chloride complex than in the bromide, because of its larger chemical shift difference between the solution and the solid. The vibrational spectra of this solid, $TlCl_3 \cdot 4H_2O$, also give a deviating behavior, see Assignments of Vibrational Spectra above, which may be due to differences in the hydrogen bonding and the Tl−O distances for the TlX_3 species in solution and in the solid state. No solid phase that contains $Tl(CN)_3$ complexes is known.

In conclusion, the available data support a trigonal-bipyramidal structure $TlX_3(OH_2)_2$ for the bromide complex and presumably also for the chloride complex in solution, while a

pseudotetrahedral $Tl(CN)_3(OH_2)$ structure seems most likely. For the isoelectronic mercury(II) ion, pyramidal HgX_3 (X = Br, I) species, probably slightly flattened pseudotetrahedral $HgX_3(OH_2)$ complexes, have been found in aqueous solution.[51] The shortening of the Hg−Br distance from $HgBr_4^{2-}$ to $HgBr_3^-$ is *circa* 0.03 Å to be compared with 0.04−0.05 Å from $TlBr_4^-$ to $TlBr_3$ (Tables 3 and 5).

TlX_4^-. The previous evidence,[7,8,13−16] showing tetrahedral symmetry for the tetrahalo complexes, is corroborated by the results obtained in this work. The Tl−X distances are 2.43, 2.56, 2.77, and 2.19 Å for X = Cl,[15] Br,[14], I,[52] and CN (this work), respectively. For the $Tl(CN)_4^-$ complex, the tetrahedral symmetry is expected considering that tetrahedral $M(CN)_4$ complexes are formed by many other d^{10} ions, *e.g.*, copper(I), silver(I), zinc(II), cadmium(II), and mercury(II).[47,48,53] The Tl−C−N coordination is linear as it is in all the cyano thallium(III) complexes studied. A similar coordination of the cyano ligands has been found for the tetrahedral $Hg(CN)_4^{2-}$ ion in the solid compound $BaHg(CN)_4{\cdot}4NC_5H_5$ where the angle Hg−C−N is ~176°.[54]

TlX_5^{2-}. In aqueous solution with sufficiently high free chloride concentration some amount of the $TlCl_5^{2-}$ complex is formed. The coordination geometry is probably octahedral, $TlCl_5(OH_2)^{2-}$, as indicated by the IR/Raman data (see Assignments of Vibrational Spectra above). Unfortunately, the structure of this complex is not accessible by X-ray diffraction/EXAFS methods, since it never dominates in aqueous solution.[7]

TlX_6^{3-}. The complex $TlCl_6^{3-}$ is formed both in aqueous solution and in the solid state. Its structure is octahedral as shown from the IR/Raman and X-ray diffraction data;[13,15] the Tl−Cl bond distance is 2.59(1) Å.

Comparison between the Thallium(III) and Mercury(II) Complexes

It is remarkable that the Tl−Cl and Tl−Br bond lengths in the first and second hydrated thallium(III)−halide complexes are virtually the same. At the formation of the first complex the halide ion replaces one water molecule, with only a slight lengthening of the mean $Tl-OH_2$ bond distance to the remaining water ligands. When the second complex is formed, the entering halide ion substitutes the water molecule *trans* to the halide ion without significant change in the thallium−halide bond lengths, but the $Tl-OH_2$ bond distance increases with about 0.1 Å (Table 3). The tendency toward linear coordination is much stronger for mercury(II) as shown from a comparison of the bond distances. The mean M−O bond length (obtained by LAXS methods) for the hexahydrated mercury(II) ion in solution, 2.41(1) Å,[22] is longer than that for the isoelectronic thallium(III) ion, 2.235(5) Å,[14] as expected for the lower charge in these electrostatically dominated ion−dipole bonds. For the second halide complexes, HgX_2 and TlX_2^+, the Hg−X bonds are *shorter*, 2.29(2) and 2.42(2) Å,[42] than the Tl−X, 2.39(2) and 2.50(2) Å, both for X = Cl and Br, respectively. For the tetrahedral HgX_4^{2-} and TlX_4^- complexes in aqueous solution the Hg−X bond distances are again longer, 2.47(1)[55b] and 2.610(5) Å,[51] than the corresponding Tl−X bonds, 2.43(1) and 2.564(5) Å, for X = Cl[15] and Br,[14] respectively.

A relatively strong hydration is found for the $TlX_2(OH_2)_4^+$ complexes with Tl−O bond distances of *circa* 2.33 and 2.31 Å for X = Cl and Br, respectively, while the uncharged HgX_2 species are weakly solvated as shown by comparison of the Hg−Cl and Hg−O bond lengths for solvated $HgCl_2$ complexes. EXAFS and LAXS studies of the $HgCl_2$ complex in aqueous and methanol solutions showed weak hydration with distinct Hg−Cl distances at 2.29(2) and 2.31(1) Å, respectively, and diffuse Hg−O interactions at about 2.7 Å.[42,55] In dimethyl sulfoxide, a slightly stronger solvation is found (Hg−Cl 2.32(2) and Hg−O 2.65(5) Å),[56] shown in a more sensitive way by the decrease in the Hg−Cl stretching vibrational frequencies.[21]

The same tendency with very strong bonds for the second mercury(II) complexes is also evident from EXAFS studies of the linear $Hg(CN)_2$ species in aqueous solution giving a Hg−C bond distance of 2.04(2) Å,[42] while the corresponding bond distance in the hydrated $Tl(CN)_2^+$ complex is 2.11(2) Å (*cf.* Table 5). The Tl−O bond distance of 2.42(4) Å shows the hydration to be fairly strong, while Hg−O distances could not be discerned. For the $Hg(CN)_4^{2-}$ complex in the solid state the mean metal−carbon bond distance is 2.20 Å,[54] while for the $Tl(CN)_4^-$ complex the corresponding distance is 2.19(2) Å.

Acidity and Water Coordination

The $Tl(OH_2)_6^{3+}$ ion is a strong acid in aqueous solution, pK_a = 1.14 (in 3 M $NaClO_4$),[6,28] the most acidic of all three-valent metal ions.[2] It splits off up to two protons, before precipitating as Tl_2O_3 on further hydrolysis. Moreover, the $TlCl^{2+}$ complex is still a strong acid, with pK_a = 1.8,[6] whereas $TlCl_2^+$ is not. These facts, together with the above mentioned results of a Raman study,[18] led to the suggestion that in a solution without complexing agents only two water molecules are strongly bonded to the Tl^{3+} ion.[6,58]

Seemingly, this proposal is not compatible with the hydration number of 6 obtained from LAXS[14] and EXAFS (this work) data for concentrated acidic aqueous solutions of thallium(III) perchlorate. A regular octahedral entity was found in the crystal structure of $[Tl(OH_2)_6](ClO_4)_3$.[27] The Tl−O distance, 2.23 Å, is somewhat uncertain (because of the large correction for "riding" motion, from 2.17(2) Å) and is not significantly different from the solution values, 2.235(5) Å (LAXS)[14] and 2.21(2) Å (EXAFS).

For mercury, the Hg−O bond distance in the crystal structure of $[Hg(OH_2)_6](ClO_4)_2$ is 2.341(6) Å (2.35 Å after a thermal "riding" motion correction).[59] The corresponding LAXS value in aqueous solution, 2.41(1) Å, is significantly larger and also shows an anomalously large Debye−Waller factor.[22,25] An analysis based on theoretical calculations explained these observations as due to second order Jahn−Teller effects, leading to dynamic distortions of the octahedral configuration.[25] In a similar vein, our preliminary results from EXAFS studies on acidic mercury(II) perchlorate solutions indicate a much shorter (ca 0.1 Å) mean Hg−O bond length than the LAXS value. A similar, but smaller effect is observed for hexahydrated Tl^{3+} (see above), and the different mean values obtained with the two methods are probably a result of the different weighting of the contributions from the short distinct and long diffuse M−O distances in the two techniques (due to failure of the harmonic potential approximation). Thus, we propose that there are two groups of M−O distances around the hexahydrated Hg^{2+} and

(51) Sandström, M.; Johansson, G. *Acta Chem. Scand., Ser. A* **1977**, *31*, 1196.
(52) (a) Glaser, J.; Goggin, P. L.; Sandström, M.; Lutsko, V. *Acta Chem. Scand., Ser. A* **1982**, *36*, 55. (b) *Ibid.* **1983**, *37*, 437.
(53) Sharpe, A. G. In *Comprehensive Coordination Chemistry*; Wilkinson, G., Gillard, R. D., McCleverty, J. A., Eds.; Pergamon: Oxford, England, 1987; Vol. 2, p 10.
(54) Brodersen, K.; Beck, I.; Beck, R.; Hummel, H. U.; Liehr, G. Z. *Anorg. Allg. Chem.* **1984**, *516*, 30.
(55) (a) Sandström, M. *Acta Chem. Scand., Ser. A* **1978**, *32*, 627; (b) **1977**, *31*, 141.
(56) Persson, I.; Penner-Hahn, J. E.; Hodgson, K. O. *Inorg. Chem.*, submitted.
(57) Thiele, G.; Bauer, R.; Messer, D. *Naturwissenschaften* **1964**, *61*, 215.
(58) Cotton, F. A.; Wilkinson, G. *Advanced Inorganic Chemistry*, 5th ed.; Wiley: New York, 1988; p 215.
(59) Johansson, G.; Sandström, M. *Acta Chem. Scand., Ser. A* **1978**, *32*, 109.

Tl^{3+} ions in solution due to second order Jahn–Teller effects, with a much more pronounced splitting for the mercury(II) ion. Further investigations are in progress.

The present results, together with the literature data, lead to another explanation of the acidity of hydrated thallium(III) complexes. Upon the formation of the first complex with OH^-, Cl^-, Br^-, or CN^- as ligands, according to the reaction

$$Tl(OH_2)_6^{3+} + X^- \rightleftharpoons TlX(OH_2)_5^{2+} + H_2O$$

the coordination of the remaining five water molecules is only slightly weakened, corresponding to the retained high acidity. The comparable pK_a values of the Tl^{3+}, $Tl(OH)^{2+}$, $TlCl^{2+}$, and $TlBr^{2+}$ species are 1.2,[60c] 1.4,[60a] 1.4[60b] and 1.8,[61] respectively, in 3 M $LiClO_4$ ionic medium, showing the greatest reduction of acidity for the softest ligand Br^-. When a second ligand is coordinated, however, the Tl–X bond strength remains high especially when both *trans* ligands are soft, while the remaining four water molecules become much more weakly coordinated (*cf.* Tables 3 and 5) and lose their acidic properties. This comparison implies that coordination of *two* soft ligands is necessary for an appreciable enhancement of the bonds in the *trans* X–Tl–X unit and that this effect is small with one hard *trans* ligand (*e.g.*, water).

For mercury(II), the hydrated HgX^+ species are *more* acidic than the $Hg(OH_2)_6^{2+}$ ion (except for X = I), although a substantial reduction of the overall hydration is observed already at the formation of the first mercury(II)–halide complex (as indicated by thermodynamic data).[62] The pK_a values are Hg^{2+} 3.6, $HgOH^+$ 2.6, $HgCl^+$ 3.1, $HgBr^+$ 3.5, and HgI^+ 4.0.[63] Thus, decreasing hardness[64] (increasing polarizability) of the ligand X evidently decreases the acidity of the *trans* water molecule. This may be due to increasing covalency of the M–X bond and weaker bonding of the *trans* water ligands. The high acidity of the $HgX^+(aq)$ species relative to that of the $Hg(OH_2)_6^{2+}$ ion is an effect partly of the decrease of the coordination number from 6 to 2 strongly coordinated ligands and partly of the high stability of the XHg(OH) complexes. The influence on the acidity of the negative ligands follows the same trend, but is less pronounced for Tl^{3+} where the six-coordination is retained upon the formation of the $XTl(OH)^+$ species.

Acknowledgment. The continuing support of the Swedish Natural Science Research Council, a grant from Carl Tryggers Foundation, and a grant from Skandinaviska Enskilda Banken for purchase of the FT-IR spectrometer are gratefully acknowledged. The EXAFS measurements were performed at the Stanford Synchrotron Radiation Laboratory (SSRL), supported by the U.S. Department of Basic Energy Science, Division of Chemical/Material Science, and the National Institutes of Health, Biomedical Resource Technology Program. Dr. Britt Hedman's expertise and excellent organization of the XAFS experimental stations at the SSRL have been highly appreciated. We are grateful to Dr. Peter L. Goggin, University of Bristol, for many stimulating discussions and assistance with preliminary vibrational spectroscopic measurements, Dr. Imre Togh, University of Debrecen, for preparation of the $KTl(CN)_4(s)$ salt, Prof. Robert A. Scott, University of Georgia, for providing us with the XFPAKG program package, and Drs. Graham N. George and Ingrid J. Pickering for the EXAFSPAK software. Mr. Ernst Hansen and Mr. Yixin Zhou are thanked for skilful technical assistance.

Note Added in Proof. After submission of this paper for publication the crystal structure of $KTl(CN)_4(s)$ has been determined.[65] In the tetrahedral $Tl(CN)_4^-$ complexes the Tl–C distance was found to be 2.20(2) Å, in agreement with the corresponding value, 2.19(2) Å, determined in the present work (Table 3).

Supplementary Material Available: Experimental reduced intensity functions for solutions with $Tl(CN)_2^+$ or $Tl(CN)_4^-$ dominating (Figure S1), EXAFS model fitting of $TlX_3(OH_2)_2$ and TlX_4^- (X = Cl and Br) and contributions from Tl–O and Tl–X distances (Figure S2), Fourier transforms for solutions of $TlCl(OH_2)_5^{2+}$, $TlCl_2(OH_2)_4^+$, $TlCl_3(OH_2)_2$, and $TlCl_4^-$, not corrected for the phase shift (Figure S3), Fourier transforms for solutions of $TlBr(OH_2)_5^{2+}$, $TlBr_2(OH_2)_4^+$, $TlBr_3(OH_2)_2$, and $TlBr_4^-$, not corrected for the phase shift (Figure S4), and first derivatives of absorption edges (XANES spectra) after calibration and normalization for TlX_n^{3-n} (solution) and TlX_4^- (solid state) (Figure S5) (9 pages). This material is contained in many libraries on microfiche, immediately follows this article in the microfilm version of the journal, can be ordered from the ACS, and can be downloaded from the Internet; see any current masthead page for ordering information and Internet access instructions.

JA943389X

(60) (a) Kul'ba, F. Y.; Yakovlev, Y. B.; Mironov, V. Y. *Zh. Obshch. Khim.* **1964**, *9*, 2573; (b) **1966**, *34*, 1003. (c) Yakovlev, Y. B.; Kul'ba, F. Y.; Mironov, V. Y. *Probl. Sovrem. Khim. Koord. Soedin. (Izd. Leningradskovo Universiteta)* **1968**, *2*, 241.

(61) Yakovlev, Y. B.; Kul'ba, F. Y.; Mironov, V. Y. *Zh. Neorg. Khim.* **1967**, *12*, 3283.

(62) Dash, K. C.; Kinjo, Y.; Persson, I. *Acta Chem. Scand.* **1990**, *44*, 433.

(63) Ahlberg, I.; Leden, I. *K. Tek. Hoegsk. Handl.* **1972**, No. 249, 17.

(64) Pearson, R. G. *Inorg. Chem.* **1988**, *27*, 734.

(65) Ilyuhin, A. B.; Glaser, J.; Maliarik, M. A.; Toth, I. Unpublished results.